Chemical Science

ROYAL SOCIETY OF CHEMISTRY

REVIEW

View Article Online
View Journal | View Issue

Cite this: *Chem. Sci.*, 2025, **16**, 3019

Natural biomolecules for cell-interface engineering

Tong-Kai Zhang,†[a] Zi-Qian Yi,†[a] Yao-Qi Huang,*[ab] Wei Geng*[a] and Xiao-Yu Yang *[ac]

Cell-interface engineering is a way to functionalize cells through direct or indirect self-assembly of functional materials around the cells, showing an enhancement to cell functions. Among the materials used in cell-interface engineering, natural biomolecules play pivotal roles in the study of biological interfaces, given that they have good advantages such as biocompatibility and rich functional groups. In this review, we summarize and overview the development of studies of natural biomolecules that have been used in cell-biointerface engineering and then review the five main types of biomolecules used in constructing biointerfaces, namely DNA polymers, amino acids, polyphenols, proteins and polysaccharides, to show their applications in green energy, biocatalysis, cell therapy and environmental protection and remediation. Lastly, the current prospects and challenges in this area are presented with potential solutions to solve these problems, which in turn benefits the design of next-generation cell engineering.

Received 12th December 2024
Accepted 18th December 2024

DOI: 10.1039/d4sc08422e

rsc.li/chemical-science

1. Introduction

Cells are the true beginning of life, and they are also the most basic living system.[1,2] Throughout the long evolutionary process, both single-cell and multicellular organisms have evolved various ways to better adapt to harsh living environments, and survive to continue their species.[3] Among these ways, the spontaneous formation of protective nanoshells around cells or organisms is an extremely common and important process in nature.[4] The spores of some bacteria have strong resistance to adverse environments due to the increased thickness of their cell wall, which is composed of polysaccharides, proteins, enzymes and fatty acids.[5,6] Spores of *Bacillus subtilis* (*B. subtilis*) can survive under high moist heat, up to 100 °C.[7] For marine mollusks, a mineralized shell provides excellent protection against harsh environments and threats from natural enemies.[8–10] Surprisingly, tumor cells in blood can utilize fibrinogen in the microenvironment to form a fibrin shell *in situ* on their surface to escape natural killer (NK) cell cytotoxicity, thus cunningly achieving hematogenous metastasis.[11] Altogether, living organisms continuously synthesize and choose various bioactive molecules with various

[a]*State Key Laboratory of Silicate Materials for Architectures & State Key Laboratory of Advanced Technology for Materials Synthesis and Processing & School of Chemistry, Chemical Engineering and Life Sciences & Laoshan Laboratory & School of Materials Science and Engineering, Wuhan University of Technology, Wuhan, 430070, China. E-mail: weigeng@whut.edu.cn; xyyang@whut.edu.cn*

[b]*School of Engineering and Applied Sciences, Harvard University, MA-02138, USA. E-mail: yhua@seas.harvard.edu*

[c]*National Energy Key Laboratory for New Hydrogen-Ammonia Energy Technologies, Foshan Xianhu Laboratory, Foshan 528200, P. R. China*

† Tong-Kai Zhang and Zi-Qian Yi contributed to this work equally.

Tong-Kai Zhang

Tong-kai Zhang received his master's degree from Northeast Electric Power University in 2017. Currently, he is a PhD candidate at the School of Materials Science and Engineering, Wuhan University of Technology (WHUT). His current research focuses on the design and applications of artificial cells.

Zi-Qian Yi

Zi-Qian Yi received his master's degree from Wuhan University of Technology (WHUT) in 2022. Currently, he is a PhD candidate at the School of Materials Science and Engineering, WHUT. His current work includes the design and synthesis of nanocellular composites, biological interfaces and catalysis.

functions for the better survival and reproduction of their species in long-term evolution, which has inspired scientists to utilize similar functional materials to enhance natural biological cells.[12–14] Guided by these fascinating natural behaviours, making an effective composite of living cells with functional nanomaterials can enhance cell stability and endow cells with required new functions.[15–19] Therefore, for better exploration, manipulation and utilization of living cells, a non-genetic and simple strategy has been developed to construct protective and multifunctional nanoshells around cells with nanoscale materials,[20] which has been widely applied in green energy,[21–24] biological catalysis,[25–28] environmental protection and remediation,[29–32] and cell therapy (Table 1).[33–37]

Indeed, in the design process of engineering cells, the selection of functional materials must be balanced against the complexity of the cell-surface morphology and cell-surface functional groups to achieve the required functions without affecting the cell activity.[38–41] In fact, a variety of materials (inorganic materials and organic materials) have been developed with the goal of enhancing cells or endowing them with new functions. Before diving fully into natural-molecule-based cell-interface engineering, it is worth comparing purely inorganic materials, synthetic polymers, *in-situ* self-synthesized polymers and natural molecules for creating engineered cells, to give an overview of their strengths and identify key areas for improvement. Firstly, we cover the strengths and weaknesses of each material, as summarized in Fig. 1, prior to evaluating the unique accomplishments of natural molecules in creating engineered living cells. The ratings in this figure are a subjective ranking of the performance of the different types of materials in cell-interface engineering, relative to the others. The primary performance criteria include long-term stability (Fig. 1A), natural degradability (Fig. 1B), biocompatibility for living cells (Fig. 1C), potential for scaling up (Fig. 1D) and the application prospects (Fig. 1E) of cell-surface nanoshells based on purely inorganic materials, synthetic polymers, cell-surface *in-situ* self-synthesized polymers and natural molecules. Inorganic-material-based cell-surface engineering typically enhances living cells with high stability and photoelectric properties due to the excellent physical and chemical stability, optical properties and electrical properties of such materials. They include oxides (MnO_2, SiO_2 and TiO_2 nanoparticles (NPs),[42–44] carbon (graphene oxide nanosheets, carbon tubes and carbon quantum dots),[45–47] metals (Au and Pd NPs),[48–50] and salt-based materials.[51–53] However, inorganic materials directly bind to the cell surface through covalent bonds or electrostatic adsorption in cell-surface engineering, which may stimulate cells and reduce cell viability. Inorganic nanomaterials can enter the cell through endocytosis, which affects cell viability, and the stability of inorganic materials leads to their poor biodegradability, which is very important in clinical applications.[54] Organic materials are other materials widely used in cell-surface engineering, and include synthetic polymers, cell-surface *in-situ* self-synthesized polymers and natural biomolecules. Synthetic polymers are macromolecular compounds with relatively uniform molecular structures and regular repetitive structures formed by the polymerization of monomers, and have been applied in cell-surface engineering due to their stable mechanical strength, acid and alkali resistance, transparency

Yao-Qi Huang

Yao-Qi Huang got his bachelor's degree at the University of Michigan—Ann Arbor and has earned a PhD at Stanford University. He used to focus on the biophysical properties of artificial cell membranes by utilizing droplet interface bilayers. Right now, he has shifted his direction to the physics of nanofunctionalized cell interfaces.

Wei Geng

Wei Geng received his PhD from WHUT. He worked as a postdoctoral fellow at Sun Yat-sen University. He is currently working as an associate researcher at Sun Yat-Sen University. His research is aimed at the design and synthesis of biohybrid materials for energy, environment, and biocatalysis.

Xiao-Yu Yang

Xiao-Yu Yang earned his B.S. degree from Jilin University in 2000 and his joint PhD degree from Jilin University, China, and FUNDP, Belgium (co-education), in 2007. After a postdoctoral fellowship at FUNDP and "Chargé de Recherches" at the F.N.R.S. of Belgium, he is currently working as a Chair professor at the State Key Laboratory of ATMSP at WHUT, an associate at Harvard University and a senior fellow at Heinrich-Heine-Universität Düsseldorf. His research is aimed at hierarchical materials for applications in catalysis, energy, and environment.

Table 1 Summary of applications of cell-interface engineering

Applications	Cell types	Materials	Functional features	Examples
Green energy	*Shewanella oneidensis MR-1* (*S. oneidensis MR-1*) cells	CdS nanoparticles (NPs)	Improving hydrogen yield	*S. oneidensis MR-1*@CdS[21]
	Escherichia coli (*E. coli*) cells	CdS NPs	Improving hydrogen yield	*E. coli*@CdS[22]
	Chlorella pyrenoidosa (*Chlorella*) cells	Fe_{III}-doped polypyrrole (PPy)/$CaCO_3$ nanocoating	Improving hydrogen yield	*Chlorella*@PPy/$CaCO_3$ (ref. 24)
Biocatalysis	*S. oneidensis MR-1* cells	Ag NPs	Improving microbial fuel cell generation efficiency	*S. oneidensis MR-1*@Ag[25]
	Moorella thermoacetica (*M. thermoacetica*) cells	Au nanoclusters (Au NCs)	Improving CO_2 fixation	*M. thermoacetica*@Au[26]
	Saccharomyces cerevisiae (*S. cerevisiae*) cells	Tannic acid (TA)-modified InP NPs	Improving production of shikimic acid	*S. cerevisiae*@TA-InP[27]
Environmental protection and remediation	*Chlorella* cells	Glass-fiber (GF)@PVDF	Efficient high-ammonia nitrogen wastewater treatment and efficient biofouling control	*Chlorella*@GF@PVDF[29]
	Phanerochaete chrysosporium (*P. chrysosporium*) cells	ZnS NPs	Efficient removal of heavy metals Pb^{2+} and Cd^{2+}	*P. chrysosporium*@ZnS[30]
	Bacillus megaterium Y-4 (*B. megaterium*) cells	Pd^0 NPs	Efficient improved OTC degradation	*B. megaterium*@Pd[32]
Cell therapy	*Bifidobacterium longum* (*B. longum*) cells	Iron single-atom catalyst (Fe SA_{50})@C18-PEG-B@metal–organic-framework-encapsulated Fe precursor (B-SA_{50})	Efficient alleviation of intestinal inflammation and microbiota dysbiosis	*B. longum*@B-SA_{50} (ref. 33)
	Chlamydomonas reinhardtii (*C. reinhardtii*) cells	DBCO-PEG_4-NHS ester NPs (NP-robot)	Efficient treatment of acute bacterial pneumonia	*C. reinhardtii*@NP-robot[34]
	Salmonella typhimurium VNP20009 (*S. typhimurium*), *Escherichia coli 25922* (*E. coli*) cells	Glucose-polymer-conjugated and indocyanine-green-loaded silicon NPs (GPICG-SiNPs)	Efficient promotion of antitumor immune responses	*S. typhimurium*/*E. coli*@GPICG-SiNPs[35]

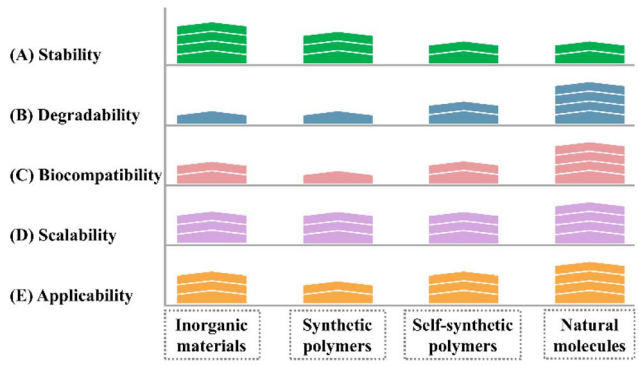

Fig. 1 Strengths and limitations of different types of material for cell-interface engineering. Each material type features inherent unique functionalities and trade-offs (A–F) in cell-interface engineering. (A) Stability represents the durability of the interface around cells, which can be evaluated from the maintenance time of the nanoshell. (B) Degradability indicates the natural degradation of the cell-surface nanoshell over a certain time, the degradation products of which can be absorbed through metabolism. (C) Biocompatibility represents the effect of the cell-surface interface on cell viability, which can be evaluated *via* the CCK-8 assay or a fluorescein luminescence approach. (D) Scalability indicates the potential of the cell-surface interface for further engineering. (E) Applicability indicates the application prospects of the engineering in comprehensive consideration of the above factors. Achieving the optimal outcome relies on the rational matching of material properties and living-cell functions. Furthermore, different levels of material engineering for living cells may be necessary, depending on the desired outcome.

and controllable modifications. They include polyethylene glycol (PEG), poly(propylene sulfide) (PPS) and polypyrrole (PPY).[55–57] However, these synthetic polymers always have problems with poor biocompatibility, reduced signal transduction and mass transport, and poor degradation performance.[58] Besides synthetic polymers, *in-situ* self-synthesized polymer-based cell-surface engineering is achieved by being directly initiated from the cell surface through controlled radical polymerization (CRP) techniques, which can alleviate the damage to living cells brought about by polymerization reactants and conditions.[58] This technology may face complex processes of engineering and require complex conditions, such as special lighting, initiators and catalysts. Thus, the application of natural active biological molecules (such as natural polyphenols, polysaccharides and proteins) for cell-interface engineering seems to be a perfect choice .[59–62] Natural active biological molecules, as perfect interfacing materials, have always been considered the best material for cell-interface engineering due to their advantages of natural biocompatibility, biodegradability, high permeability, inherent bioactivity, and diverse chemical properties, although their nanostructures are not well-defined compared to the traditional abiotic nanomaterials.[63–67] Most importantly, these natural active biological molecules are all successful cases in terms of living organisms continuously synthesizing them for the better survival and reproduction of those species in long-term

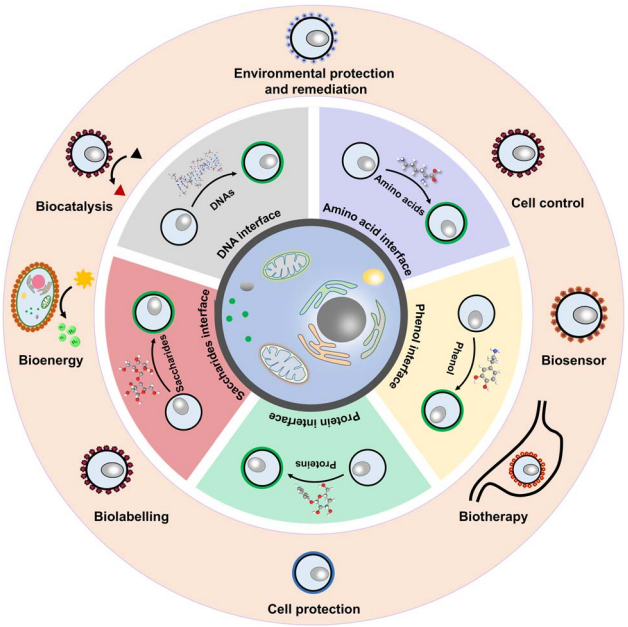

Fig. 2 A schematic showing natural biomolecular materials that are used for the creation of nanofunctionalized cells with specific nanofunctions.

evolution, meaning great feasibility in various cell-interface engineering processes.[68–71]

In this review, the progress, challenges and opportunities in cell-interface engineering are mainly discussed from the viewpoint of natural biomolecule-based functional materials for biointerfaces assembled on living-cell surfaces with augmented functionality. The natural molecules used for cell-interface engineering mainly fall into five types, including DNA (deoxyribonucleic acid) polymers, amino acids, natural polyphenols, proteins and saccharides.[72] These molecules can form different functional hybrid nanoshells around cells, with great application prospects in green energy, biocatalysts, environmental protection and remediation and cell therapy, as discussed in Fig. 2 and Table 1. Moreover, future prospects of cell-interface engineering are also provided. Finally, this review discusses presently faced challenges and provide suggestions for future research directions in this rapidly expanding area. We believe that timely information about natural-molecule-based cell-surface-engineering strategies will inspire further developments of gentler and more precise multifunctional cell-interface engineering strategies based on natural biomolecular materials.

2. Cell-interface engineering induced by a biomolecule interface

As the fundamental structural and functional units of life, biological cells have been widely exploited in devising systems for novel biotechnologies due to their unparalleled biofunctionalities.[16] However, in non-natural applications, biological cells face naturally high fragility and complex and harsh environments induce cell instability.[19] To address these issues, hybrid systems provided by cell-surface engineering can integrate the advantages of functional materials (mainly inorganic and organic materials) and living cells, endowing traditional materials with biological activity while significantly improving the stability and functionality of cells.[73] As described previously, natural biomolecules with unique characteristics and functions, such as DNA, amino acids, polyphenols, proteins and saccharides, contain a variety of functional groups that have been utilized for cell-surface engineering to create living-cell–material hybrid systems. Numerous natural active molecules have been widely exploited in developing protocols for cell-interface engineering, as illustrated in Fig. 2 and Table 2. In all cell-interface engineering approaches, the functional materials and the properties of biological cells collectively determine the resulting stability and functionality of the engineered cells. In this section, we mainly discuss natural biomolecules and biomolecule-based hybrid inorganic–organic materials (including DNA polymers, amino acids, polyphenols, proteins and saccharides) that have been developed for cell-interface engineering.

2.1 Cell-interface engineering induced by natural DNA polymers

As a naturally synthesized biopolymer and natural genetic material, deoxyribonucleic acid (DNA) is produced by the molecularly precise assembly of nucleotides with faithful replication *via* specific DNA base pairing (A-T and G-C) and the assistance of DNA-modifying enzymes; this can provide a highly tunable and specific technique for generating synthetic materials with DNA as a generic building block.[74,75] Due to its merits of reversibility, stability, biocompatibility, and biodegradability, DNA can create functional materials with high purities, controllability, specificities and affinities.[76–78] Thus, DNA polymers have been widely used in cell-interface engineering with great applications in cell–cell recognition, cell regulation and protection, and sensing of the intracellular and extracellular microenvironment.[79]

Bertozzi and co-workers demonstrated a metabolic labelling strategy to modify cells with azido sialic acid (SiaNAz) residues, which can be used for specific reaction with single DNA strands (Fig. 3A(a)).[80] Cells decorated with oligonucleotides can form 3-dimensional multicellular structures through DNA duplex formation between those cells. The rate of multicellular-structure formation is related to the density of engineered cells and cell-surface DNA. As shown in Fig. 3A(b), a decrease in cell density can lead to a decrease in the $t_{1/2}$ for the cell–cell assembly reaction. Moreover, this strategy has the ability to purify desired multicellular structures away from undesired cell structures *via* fluorescence-activated cell sorting (Fig. 3A(c)). A microtissue was constructed by the contact of a CHO cell line, labeled with green fluorescent protein and able to express the secreted growth factor interleukin-3 (IL-3), and the untransformed hematopoietic progenitor cell line (FL5.12), whose growth depends on the presence of IL-3 (Fig. 3A(d)). By controlling the secretion of the cytokine, the growth direction of the multicellular structures can be effectively controlled, which

Table 2 Summary of natural molecules used for cell-interface engineering

Type of natural molecule for engineering	Natural molecules	Functional features	Cell types	Ref.
DNA molecules				
	Deoxyribonucleic acid (DNA)	Precise manipulation (encoding, handling, and sorting) of encapsulated cells	*E. coli*, yeast and MCF-7 cells	82
	DNA	Protection and high viability	CCRF-CEM cells	81
Amino acids				
	L-Cysteine	Improving engineered cells' desulfurizing activity and separation efficiency	*Gordonia* sp. *WQ-01A* cells	70
	L-Cysteine	Self-repair and protective shells	Yeast cells	89
	L-Cysteine	Durable protection	Yeast cells	90
Polyphenols				
	Dopamine (DA)	Protection and post-engineering	Yeast cells	68
	DA	Improving the catalytic activity of engineered cells	*R. glutinis* cells	110
	DA	Protection and efficient multienzyme cascade-based interfacial biocatalysis	*E. coli* cells	85 and 165
	Tannic acid (TA)	Protection and controllable degradation on-demand	Yeast cells	119
	TA	Protection and controllable degradation	HeLa cells	96
	TA, gallic acid or epigallocatechin gallate	Improving the viability and stability of the biotherapeutic *B. thetaiotaomicron*	*E. coli* and *B. thetaiotaomicron* cells	120
	TA	Improving hydrogen production in seawater	*E. coli* cells	71
Proteins				
	β-galactosidase proteins	Generating essential nutrients and protection	Yeast cells	132
	Silk proteins	Biocompatible engineering and biodegradability	L929 fibroblasts and hMSCs	135
	Protamine proteins	Enhancing the activity and stability of cyanobacteria	Cyanobacterium (*Synechocystis* sp. *PCC 7002*)	10
Polysaccharides				
	Glycopolymers	Biotinylated phosphine	HeLa/Jurkat cells	145
	Glycopolymers	Phosphine probe comprising a flag peptide	Splenocyte cells	146
	Glycopolymers	Difluorinated cyclooctyne (DIFO)-fluorophore probes	Zebrafish	147
	Chitosan (CHI) and carboxymethyl cellulose	Enhancing probiotic-cell survival in the gastrointestinal (GI) tract	*Lactobacillus acidophilus* (*L. acidophilus*) cells	69
	Chitosan and alginate (ALG)	Introducing probiotic species into the GI tract	*B. coagulans* cells	61
	Anionized dextran and bovine serum albumin	Protection, long-term storage, post-engineering and heritable behavior	Yeast cells	141

can emulate cytokine-dependent immune-cell enlargement and the proliferation of tumor cells at locations of inflammation.

A supramolecular DNA frame-based biomimetic cell wall (BCW) has been designed to shield live mammalian cells, playing a role in protecting cells from physical and biological assaults (Fig. 3B(a)).[81] A DNA initiator (conjugated with cholesterol) was designed to be inserted into the cell membrane *via* a cholesterol–lipid interaction; the initiator can be used as the origin of the formation of a template *via* a coculture with solutions of two kinds of DNA monomer. The fluorescence images show that a DNA frame and a crosslinked matrix of alginate formed on the cell membrane, and the TEM images confirmed that a 70–150 nm BCW formed around cells (Fig. 3B(b)). As shown in Fig. 3B(c), the shielding enhancement

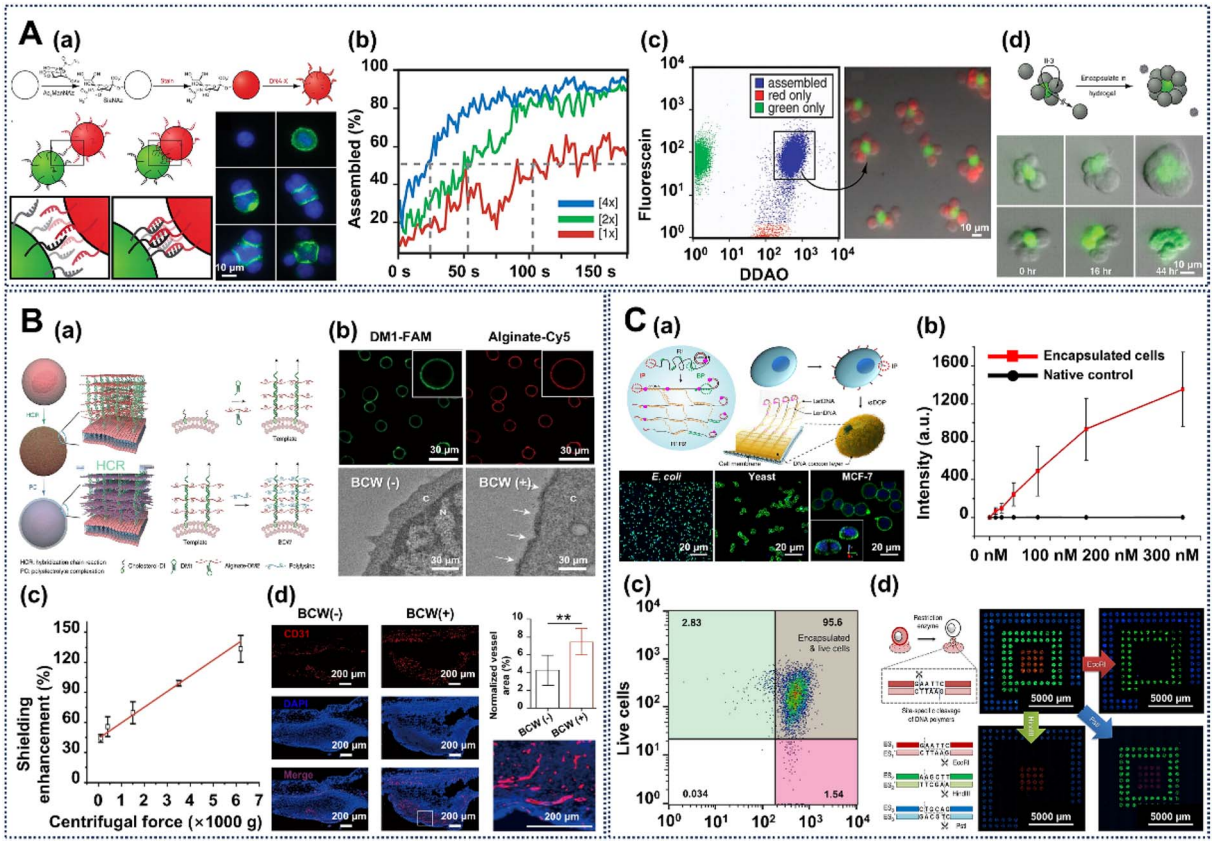

Fig. 3 Creation of engineered cell interfaces based on natural DNA polymers. (A) (a) Schematic illustration of cell-surface oligonucleotide-linked DNA polymer for forming stable cell–cell contacts, and the confocal laser scanning fluorescence microscope (CLSM) images of cells engineered with fluorescein-conjugated DNA assembled with cells with nonfluorescent complementary DNA strands. (b) The kinetic profiles of the DNA-based assembly process. (c) Fluorescence-activated cell-sorting separation of different Jurkat cell assemblies based on fluorescence properties, and fluorescence images of those isolated structures. (d) Multicellular structures of different sizes synthesized based on cell-surface DNA structures. Reproduced with permission from ref. 80. Copyright 2009, National Academy of Sciences. (B) (a) Schematic illustration of biomimetic cell wall (BCW) synthesis with DNA polymers on the cell surface. (b) Confocal fluorescence images and TEM images of the BCW template on the cell surface. (c) The relationship between the shielding enhancement and centrifugal force. (d) Staining assay of endothelial cells with an anti-CD31 antibody. Reproduced with permission from ref. 81. Copyright 2019, Springer Nature. (C) (a) Schematic illustration of *in situ* polymerization reaction with DNA polymers for cell-interface engineering and CLSM images of engineered cells. (b) The polymer density of the DNA cocoons on the MCF-7 cells through branched primers (BPs) with different concentrations. (c) The flow cytometry analysis of cell viability and the encapsulation efficiency with DNA polymers. (d) Precise handling of cells by post-editing of the DNA polymer cocoons around cells. Reproduced with permission from ref. 82. Copyright 2019, Springer Nature.

of the BCW on the cell surface linearly increases with the centrifugal force, indicating that the DNA-based BCW can protect cells in an intelligent and resilient approach for different centrifugation situations.

This biointerface can also protect the engineered cells from biological damage. An *in vivo* assay, comparing the engineered cells with native MSCs, shows that the transplanted DNA-based BCW on engineered MSCs can stimulate more angiogenesis on the transplantation sites, suggesting that the engineered MSCs release more angiogenic factors for promoting vessel formation (Fig. 3B(d)). The data demonstrates that DNA-based BCWs can protect mammalian cells from complex environmental assaults.

In another work, a DNA-orientated polymerization method was used to fabricate a DNA interface at the cell surface.[82] In this procedure, an initiating primer (IP) is attached to the cell membrane, serving as the origin of the *in situ* DNA polymerization (Fig. 3C(a)). Then, rolling circle replication guided by the IP (for synthesizing long and periodic DNA polymers) and branched replication guided by a branched primer (BP) (for generating single-stranded DNA polymers) are carried out cooperatively to complete the interface engineering of the cells, with DNA cocooning them like a fabric. The CLSM images show that the DNA-based interface engineering approach can be applied to various cells, like bacterial (*E. coli*), fungal (yeast) and mammalian cells (MCF-7) cells. The flow cytometry analysis indicates that the fluorescence intensities of the grafted DNA increase with the concentration of the IP, which implies that a controllable and well-aligned DNA interface can be obtained by adjusting the IP incubation concentration (Fig. 3C(b)). After the *in situ* DNA polymer-based cell-interface engineering, over 95.6% of the MCF-7 cells are engineered and alive, and over 80% of the cells are singly engineered (Fig. 3C(c)). This result shows that the DNA-based engineering approach is very biocompatible and highly efficient. More significantly, this

method can be used for intelligently manipulating cells. Through DNA-modifying enzymes, the DNA polymer can be manipulated with nucleotide-level precision. In this work, the encoding sequences (ESs) are selected as the cleavage sites of high-fidelity restriction endonucleases (EcoRI-HF, HindIII-HF, and PstI-HF) (Fig. 3C(d)). Thus, when incubated with those corresponding restriction endonucleases, the specific targeted DNA polymers linked with cells could be cleaved at the cleavage sites, and the designated cells could be smartly released from the capture zones of the patterned surface. In summary, the DNA-based interface-engineering method can endow cells with a functional interface, and also has great potential for controlled interactions between cells, specific assembly approaches, and precise targeted cell delivery.

2.2 Cell-interface engineering induced by amino acids

In nature, there are twenty common amino acids, and as extremely important biomolecules, these amino acids can serve as the building blocks for synthesizing peptides or proteins for living things.[83,84] Normally, amino acids have a primary amine and a carboxylic acid, and can be primed for amide, or peptide, bond formation. For proteins, the side chains of amino acids always display aromatic, polar or aliphatic groups, which are responsible for stabilizing proteins' three-dimensional and tertiary structures.[85] As typical small biological molecules, amino acids, with abundant functional groups (such as amino, carboxyl and/or thiol groups) and good biocompatibility, can display similar physicochemical properties to small organic molecules, and have been applied in fabricating specific and controllable nanostructures *via* self-assembly with nanomaterials.[85–88]

Due to their active groups, natural amino acids can very easily non-covalently bind with cell-surface groups and form a nanoshell. Therefore, our group strategically use L-cysteine as the key component in the creation of advanced biointerfaces to engineer desulfurizing bacterial living cells (Fig. 4A(a)).[70] Moreover, the biohybrids around the bacteria surface enable an active platform to stably introduce different functional nanomaterials (TiO_2 NPs, Fe_3O_4–SiO_2 nanocomposites) onto the bacteria surface (Fig. 4A(b) and (c)). Initially, we designed an L-lysine–Au biohybrid system, which can be used as an interface around desulfurizing bacteria cells for post-nanofunctionalization with TiO_2 NPs to enhance the desulfurization efficiency. As shown in Fig. 4A(d), the cell@biohybrid@TiO_2 cells have the highest desulfurizing activity in dibenzothiophene (DBT) degradation (63%), compared with cell@biohybrid cells (48%) and native cells (39%).

Subsequently, we found that hybrid coatings of L-cysteine with gold NPs can form a dynamic self-repairing artificial interface on yeast cell surfaces (Fig. 4B(a)).[89] Under this protocol, the construction of the innovative bilayered interface begins with the formation of a biohybrid layer, which is initiated by exposing yeast cells to gold NPs that are functionalized with L-cysteine molecules. During this reaction, the L-cysteine forms robust hydrogen bonds with the hydroxyl groups of polysaccharides on the yeast cell surface. This interaction results in the formation of an inner layer of the bilayered interface on the cell surfaces. The SEM, OM and TEM micrographs clearly demonstrate that the yeast cells are individually and separately engineered with an integrated interface without changing the cells' biological morphologies (Fig. 4B(b)). The EDX line confirms that the L-cysteine-modified gold-NP biohybrid, containing the Au element, are uniformly distributed around the cells. Moreover, the biological hybrid interface created in this manner has an excellent protective effect on the yeast cells under UV radiation and various culture conditions (Fig. 4B(c)). Above all, during the division of coated cells, specific hydrogen bonding interactions with L-cysteine cause deposition of gold NPs on the surfaces of daughter cells to form a supplemental interface and obtain an artificial cell with a self-repairing biointerface (Fig. 4B(d)).

Furthermore, our group found that L-cysteine can forge hydrogen bonds with the hydroxyl groups presented on the surface of the silica (Fig. 4C(a)),[90] where the interaction contributes significantly to the subsequent formation of the outer layer. By serving as a molecular bridge between these distinct layers, L-cysteine facilitates the formation of a finely structured bilayered interface. The SEM and TEM images reveal the intricate nanoscale structure of the bilayered interface (Fig. 4C(b)), which features a dense outer silica layer and a porous inner biohybrid layer. This dual-layered structure not only provides protection but also enables efficient nutrient exchange, promoting the overall health of the encapsulated cells. One of the critical aspects of this development relates to its ability to enhance the viability of yeast cells when they are exposed to a complex environment with multiple simultaneous hostile stimuli. For instance, exposure to UV radiation is known to cause DNA damage in living cells and even causes cell death. The results depicted in Fig. 4C(c) demonstrate that yeast cells engineered with the bilayered interface (depicted by the black line) maintain significantly higher viability compared to native yeast cells (depicted by the yellow line). This remarkable resilience results from a combination of factors, including nutrient storage within the interface and the absorption of UV radiation. Beyond protection, the bilayered interface can be tailored to incorporate additional functionalities, such as the integration of graphene to enhance electrical conductivity, offering opportunities for applications like bioelectrodes and cellular response monitoring. The development of this bilayered interface, composed of a biohybrid layer formed by L-cysteine-coated gold NPs and self-assembled amorphous silica, represents a ground-breaking solution for safeguarding individual *S. cerevisiae* cells against a multitude of simultaneous and hostile environmental factors. This innovation opens possibilities for a wide range of applications in biotechnology and cellular protection, and inspires us that more types of amino acids can be utilized for cell engineering.

2.3 Cell-interface engineering induced by natural polyphenol molecules

As a category of omnipresent compounds distributed in nature, polyphenols have advantages of being biocompatible, acting as

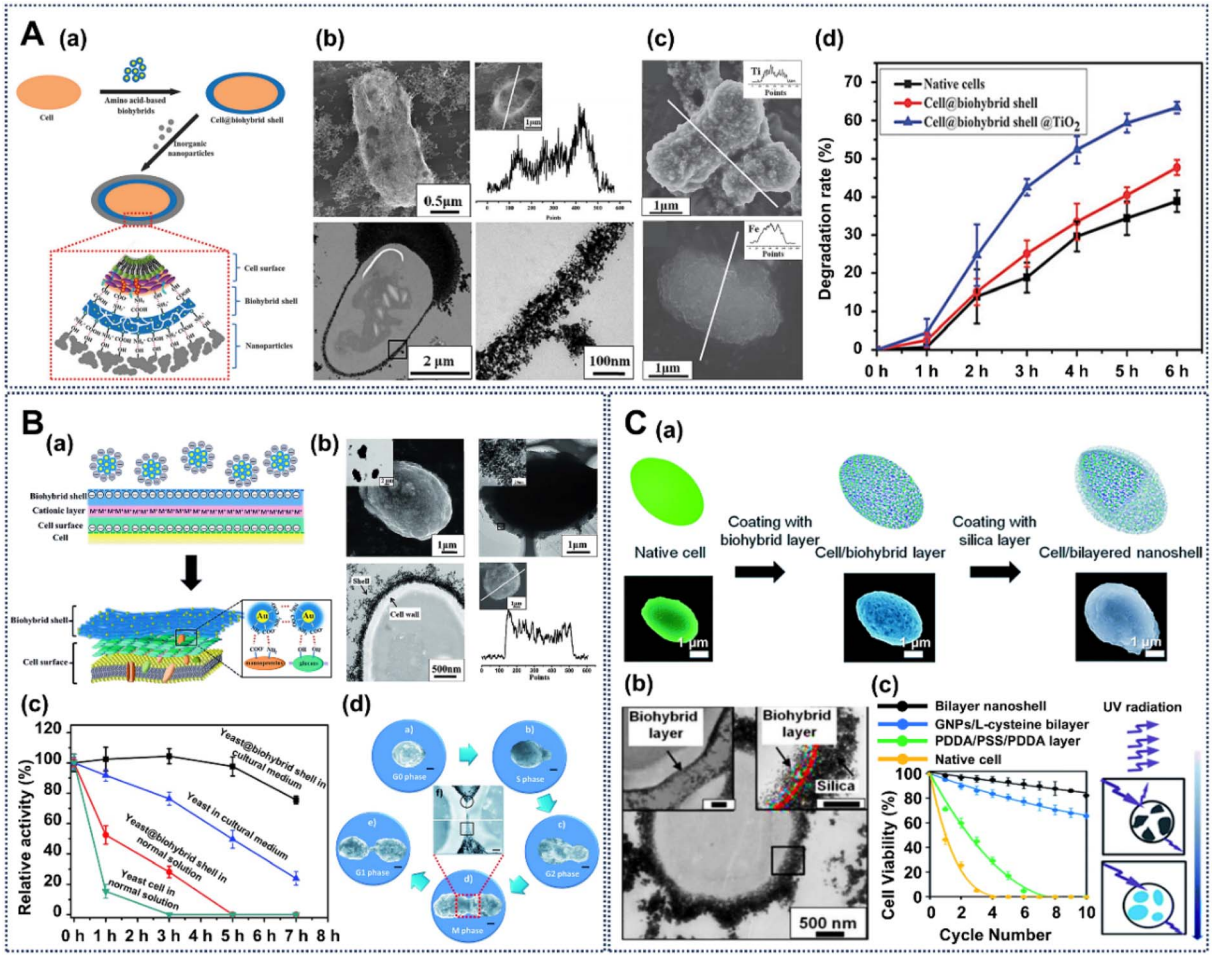

Fig. 4 Creation of engineered cell interfaces based on natural amino acids. (A) (a) Schematic of L-cysteine-based cell-surface engineering. (b) SEM and TEM images and EDX analysis of cell@biohybrid-shell@TiO_2-shell cells. (c) Post-functionalization with functional nanomaterials. (d) The desulfurizing activity of cells with different treatments. Reproduced with permission from ref. 70. Copyright 2014, Royal Society of Chemistry. (B) (a) Schematic of cell-surface engineering with L-cysteine-based biohybrids. (b) SEM and TEM micrographs of yeast@biohybrid interfaces. (c) Cell activity of biohybrid engineered yeast cells exposed to ultraviolet (UV) radiation. (d) Process of self-repairing biohybrid artificial interfaces during the whole process of cell division. Reproduced with permission from ref. 89. Copyright 2015, Royal Society of Chemistry. (C) (a) Schematic of cell-interface engineering with a bilayered interface around an *S. cerevisiae* cell. (b) TEM micrographs of a single yeast cell encapsulated with a bilayered interface. (c) Protection of bilayered-interface-engineered cells against UV radiation. Reproduced with permission from ref. 90. Copyright 2018, Royal Society of Chemistry.

biological adhesives, and having antioxidant and antibacterial activity, these properties attracting widespread attention from scientists.[91,92] All those properties are based on the unique polyphenolic structures with catechol or pyrogallol moieties, which allow strong non-covalent interactions (such as hydrogen bonding, electrostatic, and cation–π interactions) and strong covalent interactions (such as Michael addition/Schiff-base reaction, radical coupling reaction, and dynamic coordination interactions with boronate or metal ions).[93–95] Among these compounds, dopamine (DA) and tannic acid (TA) have been widely used for generation of cell-interface engineering through complex binding reactions.[96,97]

DA or 4-(2-aminoethyl)benzene-1,2-diol is an intermediate product produced by the metabolism of tyrosine through dihydroxyphenylalanine, which has been found to be present in animals and plants.[98] DA has been confirmed to have various physiological roles in human, such as neurotransmission. Therefore, under alkaline conditions, DA is easily polymerizable to form PDA with soft, adhesive and biocompatible properties; as a biological catecholamine neurotransmitter, it is also the main component of mussel adhesive proteins.[99] Above all, PDA nanocoatings show extremely strong adhesion properties due to their hydroxyl, amino, and catechol functional groups, as well as π–π interactions.[100] Thus, due to these properties, PDA has been widely used in biotechnology, such as in flexible electronic equipment and nanomedicine, where it contains an abundance of phenolic hydroxy groups.[101–103] PDA-based engineering approaches create an artificial interface that protects yeast cells, along with mammalian, fungal and bacterial cells.[104–108] The idea of using dopamine for cell-interface engineering was firstly developed by Choi and coauthors for interface engineering of yeast cells (Fig. 5A(a)).[68] In this work, polydopamine (PDA) was

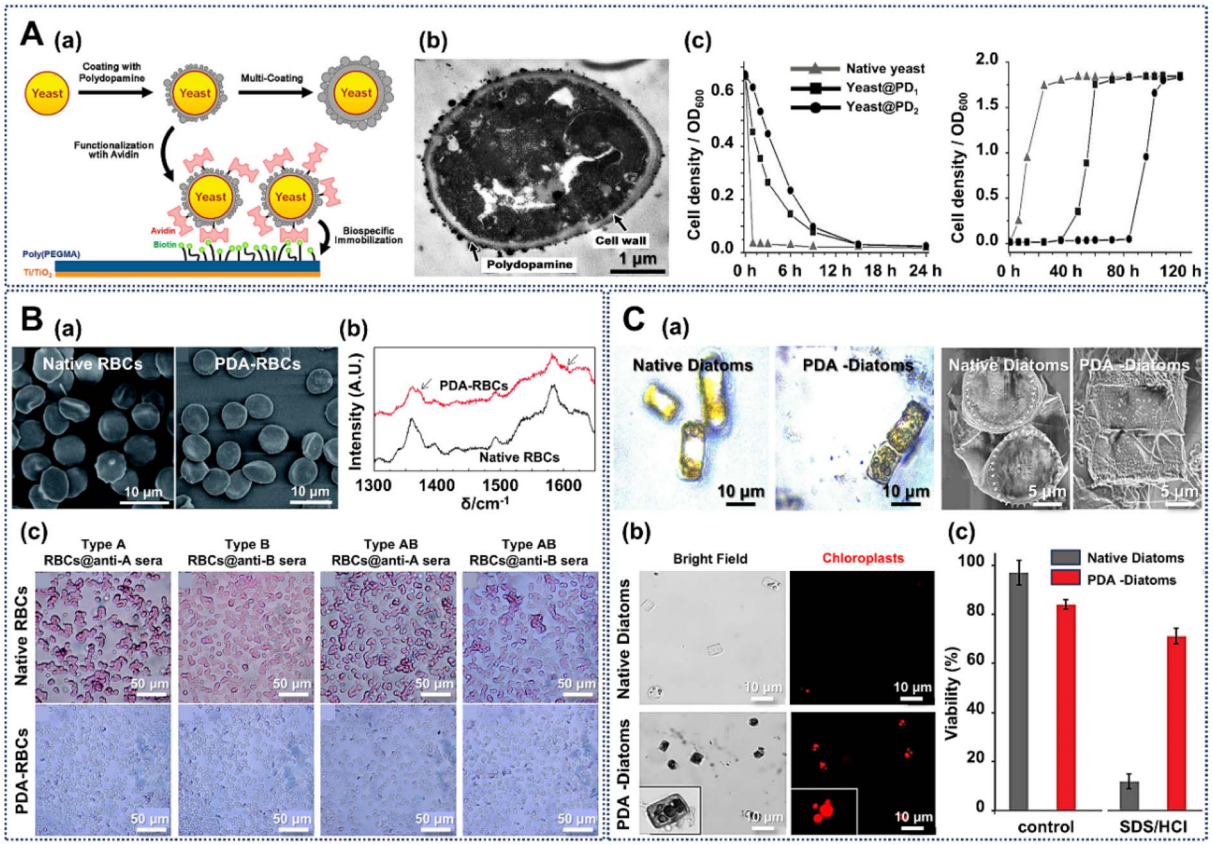

Fig. 5 Creation of engineered cell interfaces based on natural polydopamine (PDA). (A) (a) Schematic of cell-engineering procedure with PDA. (b) TEM images of the PDA-engineered yeast cells. (c) Growth curve of yeast with or without PDA engineering and protection against lyticase by the PDA interface around yeast cells. Reproduced with permission from ref. 68. Copyright 2011, American Chemical Society. (B) SEM images (a) and Raman spectra (b) of red blood cells (RBCs) without or with cell-interface engineering with PDA. (c) Antibody-mediated aggregation of human RBCs before and after PDA engineering. Reproduced with permission from ref. 104. Copyright 2014, Royal Society of Chemistry. (C) (a) Reflection microscopy and SEM images of native diatoms and diatoms with PDA engineering. CLSM images (b) and viability (c) of native diatoms and PDA-engineered diatoms after treatment with hot cleaning solutions. Reproduced with permission from ref. 109. Copyright 2022, Royal Society of Chemistry.

chosen as an engineering material for introducing an organic interface formed by strong covalent bonds, and the polydopamine interface is confirmed by TEM micrographs, which show a uniform thin film firmly coating the cell wall and big particulates (Fig. 5A(b)). The work shows that yeast cells after PDA engineering kept the capability of division, and were much more resistant against lysis than the native cells: over 70% of yeast@PD_1 (single PDA interface) and ~90% of yeast@PD_2 (double PDA interface) cells still survived after 1 h, while more than 90% of native yeast was lysed (Fig. 5A(c)). In another work, DA was also applied to block antigenic epitopes on human red blood cells (RBCs), which can be applied in creating universal RBCs in health care.[104] The SEM images show that the PDA engineering process has no significant impact on cell morphology (Fig. 5B(a)), and the Raman spectroscopy distinguishes the PDA interface formed on human RBCs (Fig. 5B(b)). Most importantly, the PDA biointerface around RBCs can effectively shield specific antigens belonging to those RBCs that can induce blood coagulation when mixed with other RBCs with anti-type antisera (Fig. 5B(c)). Besides this, DA has also been used to construct artificial nanocoatings for algal cells (diatom cells), which is proved by reflection microscopy and SEM images (Fig. 5C(a)).[109] To study the capacity of PDA as a protective nanocoating for diatom cells under different harsh environmental conditions, native diatoms and PDA-engineered diatom cells were treated with HCl (10% v/v) and sodium dodecyl sulfate (SDS, 1% v/v) solution at 55 °C. Compared with native diatom cells, with no chloroplast fluorescence after treatment with the HCl/SDS solution, the chloroplasts of the PDA-engineered diatom cells still have good auto-fluorescence, and have higher viability (~70%) (Fig. 5C(b) and (c)).

Furthermore, our group have shown that PDA can be used for cell-interface engineering for *Rhodotorula glutinis*, a whole-cell biocatalyst to produce chiral alcohols (Fig. 6A(a)).[110] In this work, the yeast cells are incorporated with a PDA interface, where the interface is formed by pH-triggered oxidative polymerization of DA monomers, which adhere on the cell wall *via* self-assembly between PDA and amine or thiol groups on the glycoproteins of cells. The TEM image confirms the nanocoating of PDA on the bacteria surface (Fig. 6A(b)). Moreover, the PDA-coated yeast cells can provide a basis to induce formation of interfaces with nanomaterials such as titanium

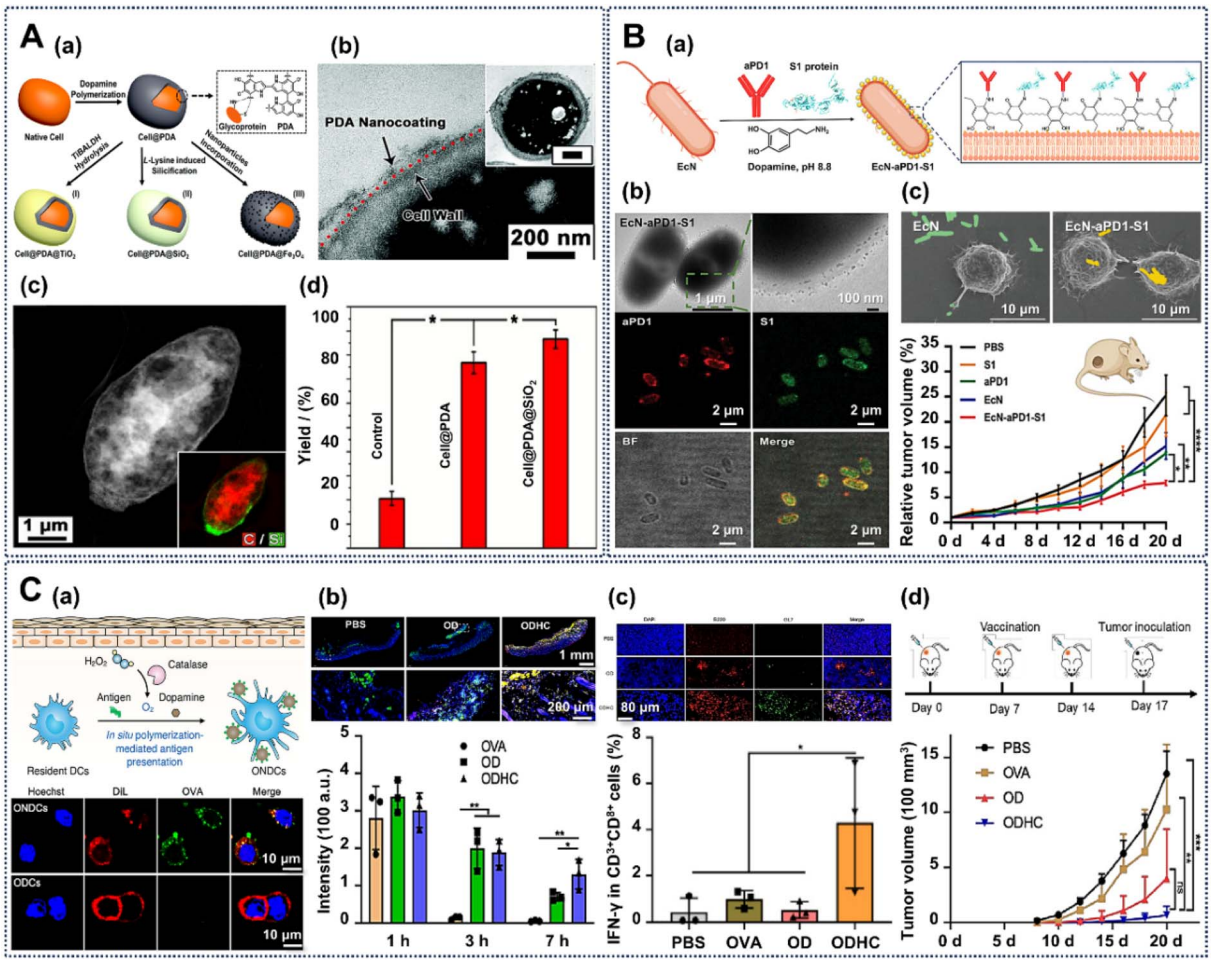

Fig. 6 Creation of engineered cell interfaces based on natural polydopamine (PDA). (A) (a) Schematic of cell engineering with PDA. (b) TEM image showing the PDA-nanocoating-engineered cells. (c) Confocal image showing the post-engineering based on the PDA interface around cells. (d) (*S*)-1-Phenylethanol yield of the native cell and engineered cells. Reprinted with permission from ref. 110. Copyright 2017, Royal Society of Chemistry. (B) (a) Schematic of PDA-engineered EcN bacteria with further modification with proteins and antibodies. (b) TEM and confocal images of the PDA-based engineered cells. (c) SEM of engineered cells targeting tumor cells and the animal experiments on mice treated with different engineered cells. Reprinted with permission from ref. 111. Copyright 2023, Wiley-VCH. (C) (a) Schematic illustration of *in situ* PDA-mediated antigen presentation on the surface of dendritic cells (DCs, top). CLSM images of ovalbumin nanovaccine-deposited DCs (bottom). (b) Fluorescence images of subcutaneous tissues (top) and quantitative analysis of mice from different treated mice (bottom). (c) Fluorescence images of inguinal draining lymph nodes (DLNs) from mice with different treatments (top), and the percentage of IFN-γ-expressing CD^{8+} T cells in the DLNs (bottom). (d) Tumor growth curves of mice throughout the immunization period. Reprinted with permission from ref. 112. Copyright 2023, American Chemical Society.

dioxide (TiO_2), silicon dioxide (SiO_2) and iron oxide (Fe_3O_4) to protect the yeast cells in harsh environments. Confocal microscopy further confirmed the post-engineering of SiO_2 NPs *via* the PDA interface (Fig. 6A(c)). The interface coated with PDA increases the catalytic activity of the yeast cells, where the yield percent of cell@PDA@SiO_2 is 4 times higher than that of the native cell (Fig. 6A(d)). These observations indicate that artificial cells can have a significantly positive effect on the catalytic efficiency of biological cells.

Recently, PDA-based cell-interface engineering has been used to functionalize *Escherichia coli* Nissle 1917 (EcN) cells for treating tumors by eliciting dual anticancer and antiviral immunity.[111] Here, PDA interfaces have been introduced on the EcN cell surface, which further allows the modification with α-PD1 and S1 protein *via* covalent bonds (Fig. 6B(a)). In this system, the α-PD1 antibody and SARS-CoV-2 spike (S1) protein are an immune checkpoint inhibitor and virus-specific antigen, while EcN cells are used as a carrier to colonize hypoxic tumor sites. The TEM image of EcN-αPD1-S1 shows that the engineered cells have the same rod shape as native EcN cells, and display a uniform PDA interface, indicating the successful engineering of the PDA biointerface (Fig. 6B(b)). Moreover, CLSM images show that the (PE)-labeled αPD1 and fluorescein isothiocyanate (FITC)-labeled S1 protein are well co-localized with EcN cells, which reveals that PDA-engineered EcN cells are efficiently decorated with αPD1 and S1 protein. The SEM images show that the PDA-based biointerface-engineered EcN cells could be captured more efficiently by DC2.4 tumor cells

than native cells (Fig. 6B(c)). Furthermore, animal experiments show that the EcN-αPD1-S1 cell-treated groups have the best inhibition of the volume of the tumor cells, which implies the activation of a humoral response by the engineered bacteria. The PDA-based functional-interface-engineered bacteria cells provide an exciting platform to design various living therapeutics for more efficient and intelligent means of cell therapy.

Moreover, previous advancements in PDA-based interface engineering show good capabilities to functionalize various cell types with precise applications.[112] Recently, Liu *et al.* proposed a strategy of PDA-based *in situ* polymerization-mediated antigen presentation (IPAP) for immunization against various diseases. The PDA-based IPAP strategy is achieved by anchoring antigen-loaded nanovaccines stably onto dendritic cells (DCs) with co-deposition with PDA *in vivo* (Fig. 6C(a), top). The CLSM images show that compared with the OVA-incubated DCs (ODCs), only the ovalbumin (OVA) nanovaccine-deposited DCs (ONDCs) show fluorescence signals around the cells, confirming the stable conjunction of OVANPs (Fig. 6C(a), bottom). The PDA-based strategy can effectively increase the efficiency of antigen presentation by DCs through improving antigen uptake and reducing lysosomal degradation. An immunofluorescence assay confirmed the *in situ* deposition of OVANPs on DCs *via* the PDA polymerization in *vivo* (Fig. 6C(b), top). The results demonstrate that PDA-based IPAP maintains prolonged localization at the injection site, with 45% fluorescence signal retention after 7 hours, indicating improved antigen stability (Fig. 6C(b), bottom). Moreover, IPAP-treated mice show a 3-fold increase in the presence of IFN-γ^+ CD^{8+} T cells, highlighting robust IFN-γ^+ CD^{8+} T cell activation (Fig. 6C(c)). Those activated CD^{8+} T cells can secrete IFN-γ, which provides good antiviral and antitumor immune responses. Compared with the control groups, the tumor growth of IPAP-treated mice was effectively suppressed, which demonstrates notable therapeutic promise (Fig. 6C(d)). These findings underscore PDA's potential to engineer different cells, which has great applications in cell protection, biocatalysis and cell therapy.

As another important natural polyphenol, TA is generally recognized as safe (GRAS) by the U.S. Food and Drug Administration. It is a mixture of polygalloyl glucose molecules with different degrees of esterification, and is widely present in various plants.[113] The polyphenol structures of TA can bind or chelate with polysaccharides, proteins, alkaloids, and metal ions, and are the main reason for the general surface binding affinity that has been used to form films on a wide variety of substrates, including different biological cells.[27,114–117] In the application of cell-surface engineering, metal–organic coordination complexes of TA–Fe_{III} can be formed *in situ* on cell surfaces. In this process, the pyrogallol (1,2,3-trihydroxybenzene) moiety in TA plays the role of a bidentate ligand for Fe_{III} and forms bis and/or tris complexes on the cell surface, which act as a protective functional nanocoating.[118]

For example, a metal–organic biointerface composed of tannic acid (TA) and Fe_{III} has been used to construct a structurally robust yet responsive biointerface around cells, amenable to controlled degradation under cytocompatible conditions (Fig. 7A(a)).[119] This TA-based interface engineering is achieved *via* the biocompatible coordination complexes of TA and Fe_{III}. The TA–Fe_{III} interface is formed by adding aqueous solutions containing fresh TA and $FeCl_3$ to an aqueous yeast suspension, creating a biointerface around cells in the mixture in only 10 s. In the FE-SEM image of native yeast cells, their surface appears smooth and intact. However, in the image of Yeast@$[TA\text{-}Fe_{III}]_4$, a distinct and well-defined interface-like structure is tightly surrounding the yeast cells (Fig. 7A(b)). This interface exhibits uniformity and is further substantiated in the TEM image of Yeast@$[TA\text{–}Fe_{III}]_4$, represented by a dark layer encircling the yeast cells with approximately 40 nm thickness. The TA–Fe_{III} interface displays remarkable protective attributes, effectively shielding the encapsulated cells from various stressors, including UV-C irradiation, lytic enzymes, and silver NPs. Fig. 7A(c) illustrates the protective potential of the TA–Fe_{III} interface against UV-C irradiation. The results indicate that when subjected to 8 J of UV-C light, 92.0 ± 0.6% of native yeast cells succumbed, while 73.1 ± 1.9% of Yeast@$[TA\text{–}Fe_{III}]_4$ cells remained viable. This underscores the capacity of the TA–Fe_{III} interface to efficiently screen and absorb UV-C radiation, safeguarding the enclosed yeast cells from its deleterious effects. Under mild conditions, such as exposure to diluted hydrochloric acid, the interface can be selectively degraded, enabling the resumption of cell division. Moreover, this pH-dependent property of the TA–Fe_{III} structure can realize reversible nanofunctionalization on the cell surface (Fig. 7B(a)).[114] After the formation of the TA–Fe_{III} interface on the cell surface, the TA–Fe_{III} interface could be removed by reducing the pH value (Fig. 7B(b) and (c)). Furthermore, SEM images and EDS analysis confirmed that this TA–Fe_{III} interface can also be used to engineer bacteria (*E. coli*, Fig. 7B(d)) and mammalian (PC12, Fig. 7B(e)) cells.

Brinker and co-workers introduced a stable and protective NP-based exoskeleton employing various NP building blocks (such as ZIF-8, SiO_2 and Fe_3O_4 NPs) on the TA–Fe_{III} interface around mammalian cells (called Supracells), which can avoid the typical endocytic nanoparticle internalization (Fig. 7C(a)).[96] For example, the formation of a ZIF-8 NP-based exoskeleton on HeLa cells mediated by a TA–Fe_{III} interface can be confirmed by the bright-field, SEM and confocal Z-stack images in Fig. 7C(b). After being functionalized with an NP-based exoskeleton, the HeLa cells have a higher viability than native HeLa cells in the presence of ROS (H_2O_2) stimuli, which is due to the antioxidant properties of the tannic acid of the TA–Fe_{III} interface (Fig. 7C(c)). The cell-surface NP-based exoskeleton displays a good resistance to pH ranging from 4–11, mainly brought about by the ion-chelating effect of the cell-surface TA–Fe_{III}-based exoskeleton framework (Fig. 7C(d)). Moreover, for different applications, NP-based exoskeletons with multifluorescent labeling, magnetism and electrical conductivity can be introduced on the cell surface as needed (Fig. 7C(e)). This TA-based biointerface holds the potential to propel the field of single-cell manipulation and chart new paths for innovative biotechnological applications.

TA and Fe_{III} represent pioneering components in the establishment of biointerfaces for cell engineering, which implies potential for other polyphenolic compounds such as gallic acid

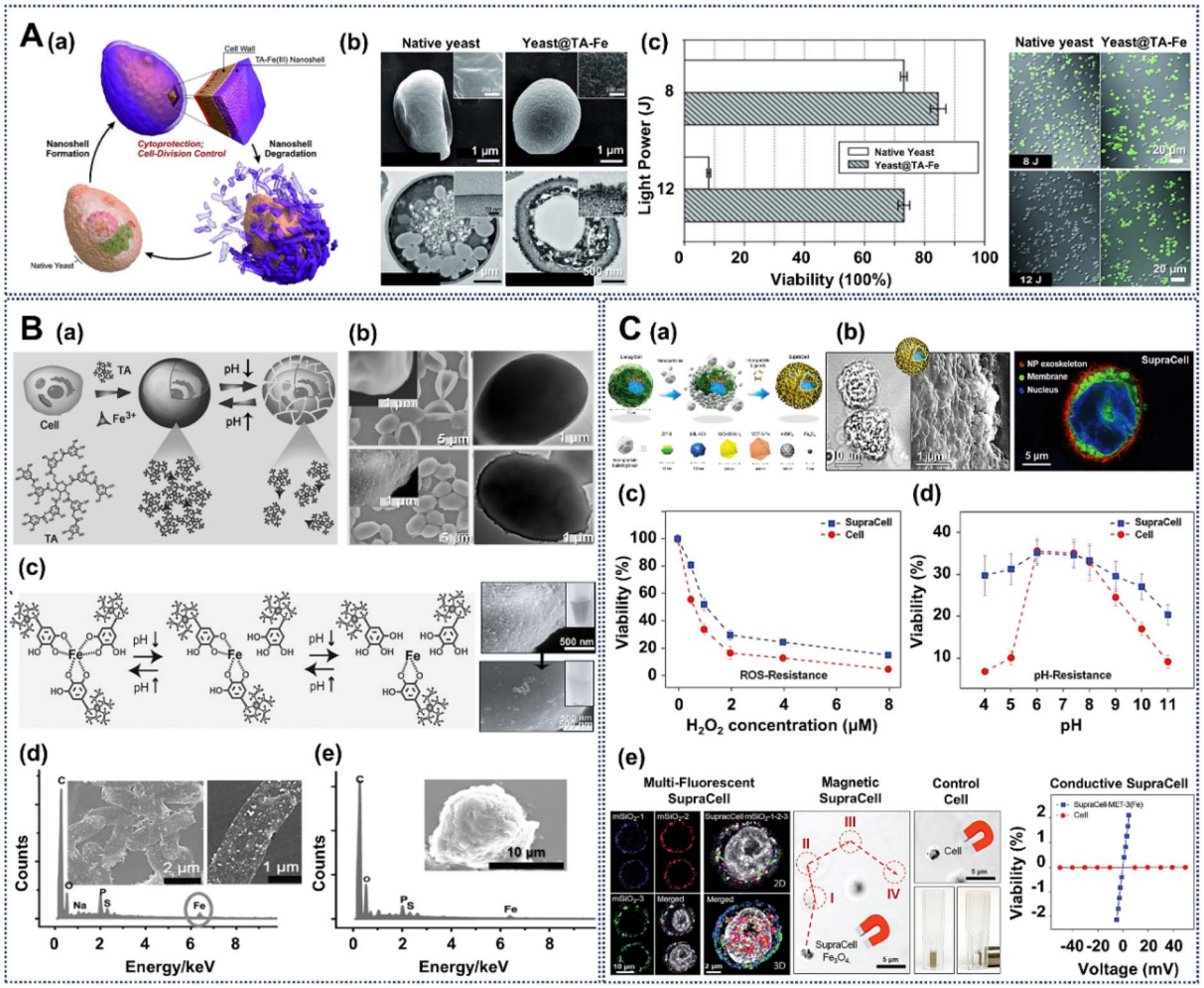

Fig. 7 Creation of engineered cell interfaces based on TA. (A) (a) Schematic of the controlled formation and degradation of TA-Fe_{III}-interface-engineered *S. cerevisiae* cells. (b) FE-SEM micrograph and TEM micrograph of TA-Fe_{III}-engineered yeast cells. (c) Protection against UV-C irradiation of the TA-Fe_{III}-engineered interface. Reprinted with permission from ref. 119. Copyright 2014, Wiley-VCH. (B) (a) The acid triggered reversible engineering of a TA-Fe_{III} interface on yeast cells. (b) SEM and TEM images of native yeast cells (top) and TA-Fe_{III}-interface-engineered yeast cells (bottom). (c) pH-dependent reversible formation of the TA-Fe_{III} interface. SEM images and EDS spectrum of *E. coli* (d) and PC12 (e) cells engineered with a TA-Fe_{III} interface. Reprinted with permission from ref. 114. Copyright 2015, Wiley-VCH. (C) (a) Schematic representation of SupraCell formation *via* immediate, TA-assisted formation of NP exoskeletons. (b) Bright-field (left), SEM (middle) and CLSM (right) images of HeLa SupraCells based on assembly of ZIF-8 NPs *via* TA interparticle ligands. Viability of native HeLa cells and SupraCells-MIL-100(Fe) against ROS stimulus (c) and pH change (d). (e) Multifluorescent labeling, magnetic, and conductive properties of SupraCells with different functional nanomaterials assembled *via* the cell-surface TA-Fe_{III} biointerface. Reprinted with permission from ref. 96. Copyright 2019, Wiley-VCH.

(GA) and epigallocatechin gallate (EGCG) to engage with metal ions, thus facilitating the formation of metal-phenol networks (MPNs).[120] Based on this point, Furst *et al.* explored different MPN biointerfaces for bacterial cell engineering. These comprise non-covalent coordination complexes of metal ions and different natural polyphenols (TA, GA and EGCG) (Fig. 8A(a)).[120] The SEM images reveal that uncoated *E. coli* cells exhibit a notably smoother surface compared to their MPN-coated counterparts, which display an augmented surface roughness (Fig. 8A(b)). Changes in the morphology of the engineered cells are a direct result of the effective formation of an MPN layer. Lyophilization, a critical step in long-term cryopreservation and long-distance transportation, affects the activity of bacteria cells and thus influences follow-up applications.[121] Furst *et al*'s work confirms that cells engineered with an MPN interface exhibit considerably higher survival rates post-lyophilization, even in the absence of traditional cryoprotectants. Furthermore, as shown in Fig. 8A(c), MPN-engineered *E. coli* and *B. thetaiotaomicron* display augmented optical density (OD) values after 48 h incubation, in contrast to control groups. Remarkably, even in the absence of conventional cryoprotectants, MPN-engineered *E. coli* suspended in phosphate citrate buffer (PC) exhibits a remarkable 3-fold increase in OD after 48 h, while *B. thetaiotaomicron* demonstrates exponential growth after 96 h, in stark contrast to the control groups, which exhibit no discernible growth (Fig. 8A(d)). The MPN-interface-based cell engineering provides a biocompatible and versatile solution with far-reaching

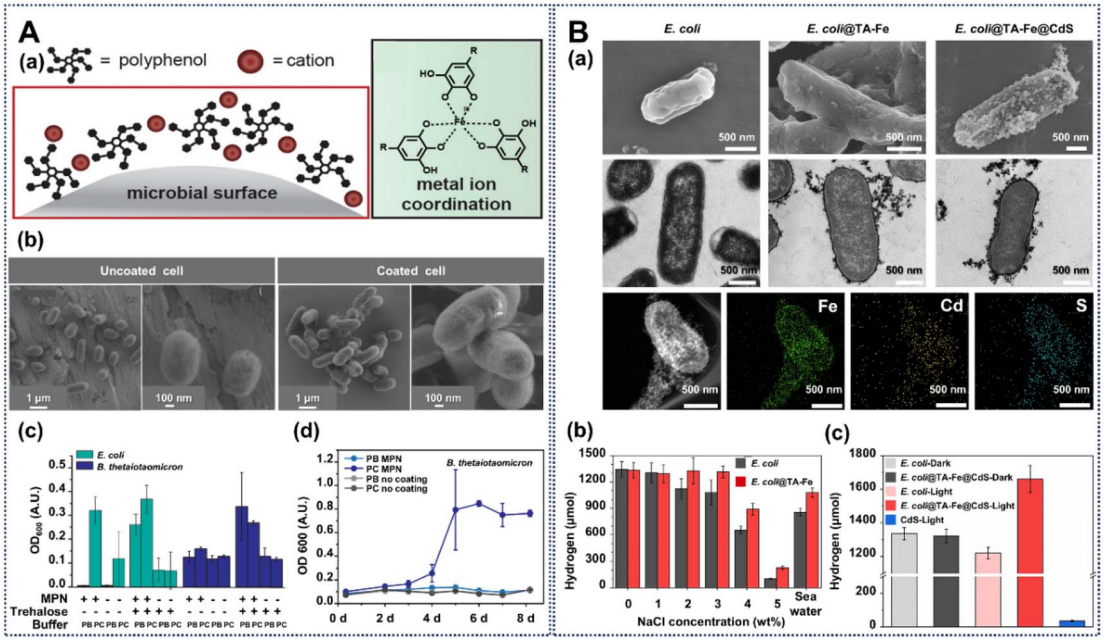

Fig. 8 Creation of engineered cell interfaces based on TA. (A) (a) Illustration of the engineering of an MPN on microbes with Fe_{III} ions and polyphenols. (b) SEM images of the MPN-engineered cells. (c) Enhanced survival and growth of MPN-coated *E. coli* and *B. thetaiotaomicron*. (d) The growth rates of native cells and MPN-coated cells. Reprinted with permission from ref. 120. Copyright 2022, American Chemical Society. (B) (a) Microscopy characterization of native *E. coli*, *E. coli*@TA–Fe_{III}, and *E. coli*@TA–Fe_{III}@CdS cells. (b) Quantitative assessment of hydrogen production by the *E. coli*@TA–Fe_{III} system and control experiments within varying salinity environments. (c) Evaluation of the hydrogen production performance of the *E. coli*@TA–Fe_{III}@CdS biohybrid system and control experiments under illumination. Reprinted with permission from ref. 71. Copyright 2023, Wiley-VCH.

implications for the development of microbial biotherapeutics, and has the potential to enable the production of a broader range of microbial strains and open new avenues for the delivery of living biotherapeutics to the gut through biointerface-engineered microorganisms.

Moreover, a TA-based biointerface can operate as an intermediary medium, facilitating adhesion of various materials to microorganisms. Utilizing the TA–Fe_{III} biological interface as a foundation, our group designed a functional biological hybrid system by attaching semiconductors (CdS NPs) to *E. coli* cells to enhance the stimulation of sustainable biological hydrogen production, especially under marine conditions.[71] SEM images confirm that the *E. coli* surface exhibits a roughened appearance while still retaining structural integrity post-encapsulation (Fig. 8B(a)). TEM images further validate the successful engineering of *E. coli* within the TA–Fe_{III} interface and corroborate the presence of CdS NPs on the cell surface. TEM elemental mapping unequivocally confirms an even dispersion of CdS NPs within the *E. coli*@TA–Fe_{III}@CdS biohybrid system. Elevated salinity levels exert a marked detrimental effect on the hydrogen production capabilities of native *E. coli*; in striking contrast, *E. coli*@TA–Fe_{III} displays notable resilience under such conditions, manifesting minimal fluctuations in hydrogen production (Fig. 8B(b)). Notably, experiments conducted within real seawater environments reveal that *E. coli*@TA–Fe_{III} continues to exhibit efficient hydrogen production, surpassing native *E. coli* performance by an impressive 26.36%. This result attests to its efficacy in safeguarding cells from the adverse effects of heightened osmotic pressures in seawater to either sustain or enhance hydrogen production. Furthermore, the TA–Fe_{III} interface facilitates the incorporation of CdS NPs onto the cell surface, which can bring more electrons. Under dark conditions, native *E. coli* and *E. coli*@TA–Fe_{III}@CdS cells exhibit comparable hydrogen production levels, indicating that CdS loading has a negligible impact on the viability and activity of *E. coli* (Fig. 8B(c)). However, under intense illumination, cell damage may occur, leading to a decline in the hydrogen-producing activity of native *E. coli* cells. In contrast, *E. coli*@TA–Fe_{III}@CdS consistently displays the highest hydrogen production levels, surpassing native *E. coli* by 36.15%. This suggests the presence of a photo-synergistic enhancement in the biohybrid system, where CdS NPs on the surface of *E. coli* amplify the catalytic activity for hydrogen generation in the presence of light. The result underscores the importance of the TA–Fe_{III} biointerface as an adhesive interface to protect cells, enhance cell-surface electron transfer and adsorb functional nanomaterials, ultimately resulting in an enhancement of hydrogen production.

2.4 Cell-interface engineering induced by natural proteins

Proteins are the material foundation of all life and the main agents of activities in living systems, and are made up of amino acids.[122] Every cell and all important components in the body involve proteins.[123,124] Moreover, proteins exhibit a variety of naturally occurring biological functions such as catalyzing

metabolic reactions, replicating DNA, responding to stimuli, and mediating molecule transportation.[125] Thus, proteins with rich functional groups seem to be worthwhile biomolecules to employ in cell-interface engineering *via* complex bonding, such as covalent and noncovalent bonding.[126,127] In fact, natural proteins have been widely used in cell-interface engineering *via* mild non-covalent bonds.[128–130]

In tissue engineering, the stability of cells is affected by physical, chemical, and environmental stimuli. To overcome these issues, Akashi *et al.* introduced a protein-based extracellular matrix (ECM) using a layer-by-layer (LbL) approach on HepG2 cell surfaces, which can provide robust protection against physical stress (Fig. 9A(a)).[131] In this process, fibronectin (FN) and gelatin (G) are sequentially layered onto the cell membrane using the LbL method, which can enhance cells' structural integrity and resilience, essential for withstanding physical stress. Moreover, growth curves indicate that FN-G-engineered cells maintain good proliferation rates, similarly to uncoated cells, and still exhibit a typical morphology, which shows the high biocompatibility of this approach (Fig. 9A(b)). Importantly, the FN-G nanocoating around the HepG2 cells displays an excellent performance in preventing physical stress-induced damage. Compared with the 6% viability of uncoated HepG2 cells, FN-G-engineered cells retained a high viability rate exceeding 85% after 18 centrifugation cycles (Fig. 9A(c)). Besides that, lactate dehydrogenase (LDH) leakage assays further revealed that FN-G-coated cells showed minimal LDH leakage, demonstrating that the protein-based nanocoating effectively preserves membrane integrity and reduces cell damage during stress (Fig. 9A(d)).

In another work, Falcaro *et al.* designed engineered yeast cells (yeast-β-gal/ZIF-8) with a functional β-galactosidase (β-gal) protein around cells, and then post-engineered them with a removable inorganic protective porous shell *via* the crystallization of a ZIF-8 metal–organic framework (MOF) film on the enzyme interface (Fig. 9B(a)).[132] In the process, the cationic β-gal protein can be adsorbed onto the anionic cell surface, and then the protein interface around the cell can attract the MOF precursors and support the rapid biomimetic crystallization to form a ZIF-8 nanoshell. In this work, bioactive exogenous enzymes (β-gal protein) are used to engineer yeast cells to generate essential nutrients, and then the proteins and cells are protected with ZIF-8 to allow the cells to survive in a hostile environment. The surface coverage is confirmed by confocal laser scanning microscopy, where the living cells can catalyze fluorescein diacetate (FDA) into fluorescein (green), β-gal was labeled with Alexa Fluor 568 (purple), and the ZIF-8 coatings were labeled by infiltration of Alexa Fluor 647 (red) (Fig. 9B(b)). From Fig. 9B(c), compared with native cells, it is obvious that the yeast-β-gal/ZIF-8 cells show higher viability in various complex and harsh environments. For instance, in long-term preservation, the viability of yeast-β-gal/ZIF-8 cells only shows a 30% decrease after 7 days under different culture conditions, while most of the native cells died (Fig. 9B(c)). Moreover, yeast-β-gal/ZIF-8 cells retain over 70% viability after 7 days with culture with lyticase or protease, while native cells show a 90% decrease on day 1. The results suggest that the engineered interface of the yeast-β-gal/ZIF-8 cells can generate essential nutrients for supplying cells, and it also can be used for protecting cells against toxic enzymes.

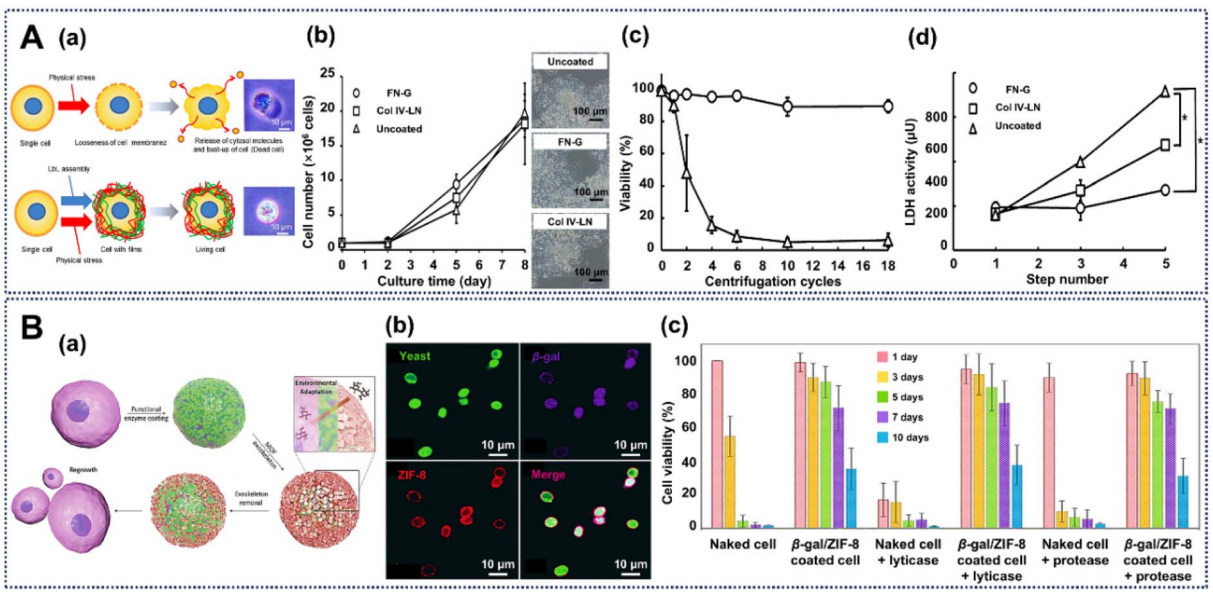

Fig. 9 Creation of engineered cell interfaces based on natural proteins. (A) (a) The layer-by-layer (LbL) assembly of a fibronectin-gelatin (FN-G) biointerface on a human hepatocyte carcinoma (HepG2) cell surface to protect against physical stress. (b) Growth curves and phase-contrast images of HepG2 cells with different treatments after 8 days of culture. Viability of HepG2 cells with or without protein-based engineering against centrifugation (c) and lactate dehydrogenase (d) stresses. Reprinted with permission from ref. 131. Copyright 2013, American Chemical Society. (B) (a) Schematic of cells functionalized with β-gal and ZIF-8. (b) CLSM images of the β-gal and ZIF-8 engineered cells. (c) Protection from the β-gal and ZIF-8 hybrid nanocoating around cells in long term survival, and lyticase and protease environments. Reprinted with permission from ref. 132. Copyright 2017, Wiley-VCH.

Silk fibroin has wide applications in tissue engineering, regenerative medicine, drug delivery and medical devices due to its advantages of great biocompatibility and good mechanical and physicochemical properties (such as good flexibility and tensile strength, breathability and moisture permeability).[128,133,134] Thus, researchers have used modified silk fibroin to design engineered cells.[135] In this procedure, aminated silk and carboxylated silk proteins are designed to form an interface on mammalian cells using a layer-by-layer (LbL) assembly approach *via* electrostatic interactions, which can be confirmed by CLSM images (Fig. 10A(a)). As we can see from the CLSM images in Fig. 10A(b), the silk-based interface around cells shows good cytocompatibility, where the cell viability is not significantly different from that of the respective control groups. Furthermore, the metabolic activity estimated from the percent reduction of Almar Blue gradually increased over 8 days for both control and engineered cells, suggesting cell proliferation (Fig. 10A(c)). Dye reduction by silk-based engineered cells is significantly lower than that by the control cells at days 1 and 3, indicating lower metabolic activity and proliferation at early time points.

Recently, our group designed a protein-based interface system by introducing an ordered silicon interface around cyanobacterium cells (*Synechocystis* sp. PCC 7002).[10] In this procedure, anionic cyanobacterium cells are engineered with cationic protamine to form a biointerface that can be used as an electrostatic template to obtain an ordered packed silica nanoshell with organized, uniform and tunable nanoporosity (Fig. 10B(a)). The complex ordered silica nanoshell induced by the protein interface around the cells can be confirmed by SEM micrographs, EDX mapping, CLSM micrographs and TEM micrographs (Fig. 10B(b)).

The engineered interface affects the growth kinetics with an increasing lag-time, but the growth rates of cell@protamine@ordered SiO_2 (cell–ordered yolk–shell) shows the same trend as native cells (Fig. 10B(c)). In applications, the ordered-yolk–shell allows the cyanobacteria not only to maintain the regular biological activity of native cells at low photon flux densities, but also to exhibit significantly enhanced biological activity at higher photon flux densities as well (Fig. 10B(d)).

2.5 Cell-interface engineering induced by natural polysaccharides

Polysaccharides are a class of complex and large carbohydrate substances formed by the condensation and dehydration of multiple monosaccharide molecules, which are widely distributed and important in nature.[136] Polysaccharides have various functions in living organisms, where peptidoglycans and cellulose can make up the cell walls of bacteria and plants, glycogen can be used as a nutrient store in animals and plants, and heparin has a good anticoagulant effect.[137] As natural polymers, polysaccharides have been proven to be highly stable, nontoxic, hydrophilic, modifiable and biodegradable. Particularly, the hydrophilic groups of polysaccharides can interact with biological tissues in a noncovalent manner to enable high bioadhesion.[138–140] Due to the advantages mentioned above, saccharides, such as chitosan and carboxymethyl cellulose, have been widely used in cell-interface engineering.

For example, Raichur and coworkers provide a cell-interface engineering method by layer-by-layer (LbL) self-assembly of chitosan (CHI) and carboxymethyl cellulose (CMC) on the cell surface of the probiotic *Lactobacillus acidophilus* (*L. acidophilus*), which displays negative charge due to the ionized acid groups on the cell wall (Fig. 11A(a)).[69] The images in Fig. 11A(b) show

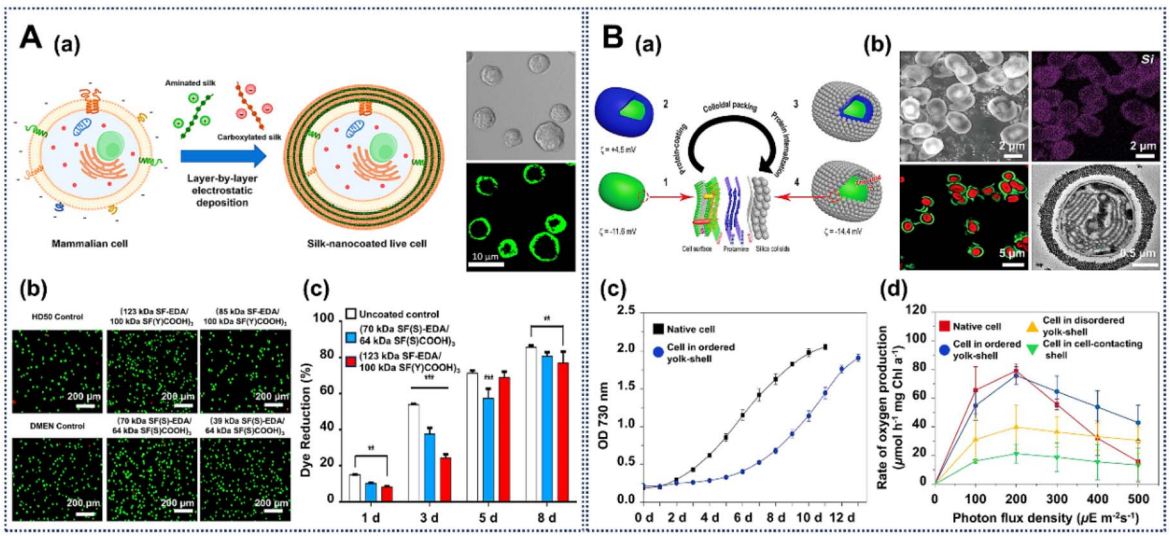

Fig. 10 Creation of engineered cell interfaces based on natural proteins. (A) (a) Schematic of mammalian cells engineered with aminated and carboxylated silk protein. (b) Fluorescence microscopy shows the cell viability of the silk-engineered cells. (c) Dye reduction rate of native and engineered cells. Reprinted with permission from ref. 135. Copyright 2020, American Chemical Society. (B) (a) Schematic of engineered cyanobacteria cells and post-functionalization with a silicon compound. (b) CLSM and TEM images indicate the success of the introduction of a silicon hybrid coating on the cyanobacteria. (c) The cell growth of the native and engineered cells. (d) Photosynthetic activities of native and engineered cyanobacteria, measured *via* oxygen production. Reprinted with permission from ref. 10. Copyright 2021, Oxford University Press.

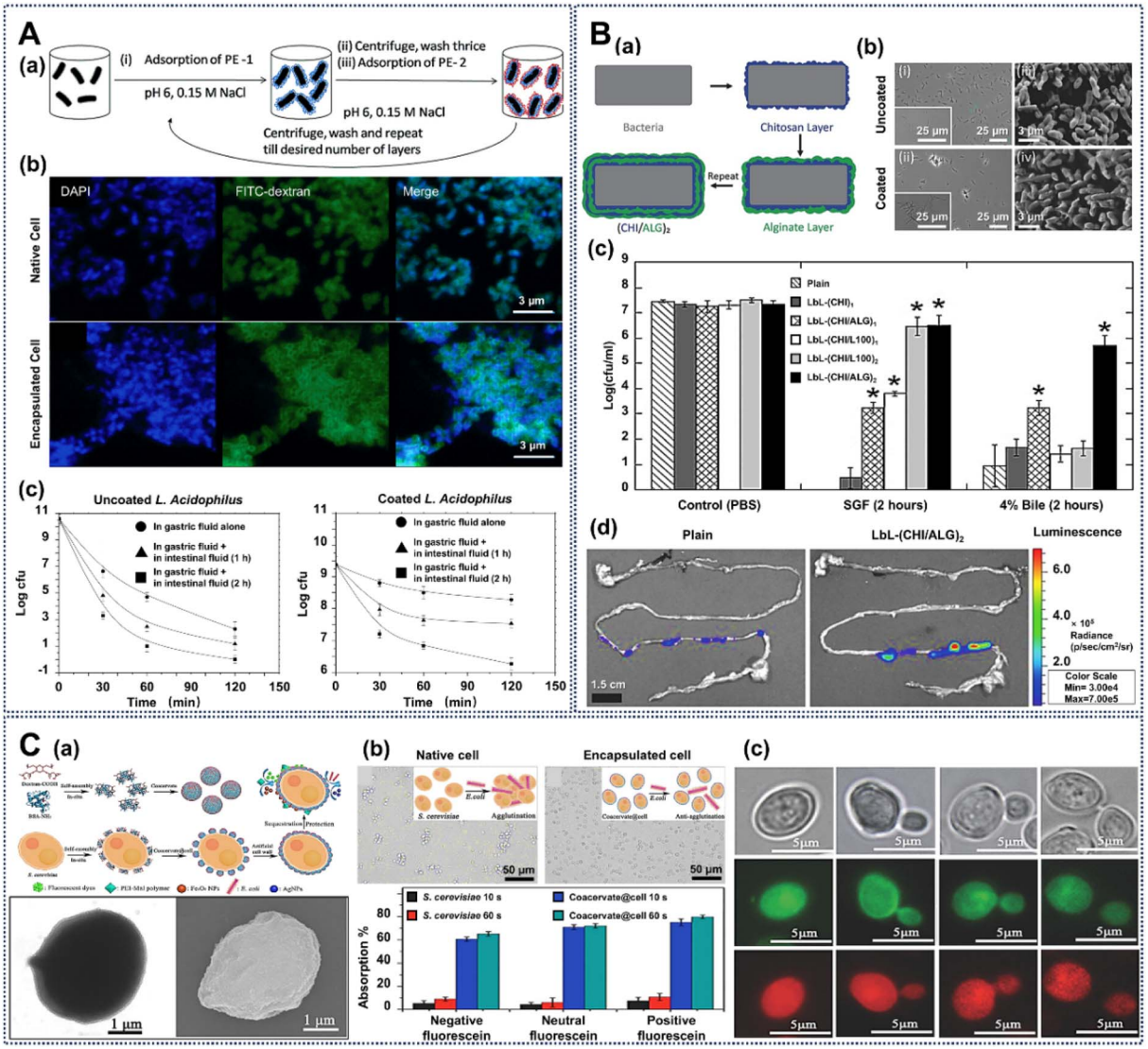

Fig. 11 Creation of engineered cell interfaces based on polysaccharides. (A) (a) Schematic of LbL assembly of polyelectrolytes of chitosan (CHI) and carboxymethyl cellulose (CMC) on bacterial cells walls. (b) CLSM micrographs of native and engineered *L. acidophilus* cells. (c) Survivability of native and engineered *L. acidophilus* in simulated gastric and intestinal conditions. Reprinted with permission from ref. 69. Copyright 2011, American Chemical Society. (B) (a) Schematic of LbL assembly of chitosan and alginate on a probiotic. (b) Bright-field and SEM images of uncoated-BC (*Bacillus coagulans*) and LbL-$(CHI/ALG)_2$-BC cells. (c) Effect of LbL coatings on probiotic survival against acid and bile insults. (d) Representative *in vivo* imaging system (IVIS) images of plain-BC and LbL-BC after 1 h oral gavage. Reprinted with permission from ref. 61. Copyright 2016, Wiley-VCH. (C) (a) Procedure of the fabrication of a coacervate-based engineered artificial cell wall around cells (top) and TEM and SEM images of a coacervate-coated *S. cerevisiae* cell (bottom). (b), *E. coli*-induced agglutination assay (top) and the adsorption ability of native or engineered *S. cerevisiae* cells toward fluorescein after different times (bottom). (c) CLSM images of the engineered cells at different budding stages. Reprinted with permission from ref. 141. Copyright 2018, Wiley-VCH.

that in the native cells, the blue (DAPI) and green (FITC) fluorescence is found throughout the whole cells. But in the LbL-engineered cells, the blue fluorescence is basically inside the cell and the green fluorescence of FITC is around the cell surface. This indicates that the native cells can easily take up DAPI and the FITC-dextran, while the engineered cells can only take up DAPI and inhibit the larger FITC-dextran molecules, showing a selective permeability to molecules with different sizes. Thus, as shown in Fig. 11A(c), the number of native cells is reduced from 10.4 log cfu per 500 mg to 4 log cfu per 500 mg when cultured in simulated gastric fluid (SGF) for 120 min. Meanwhile, under the same conditions, the engineered cells just show a slightly decrease, where the number of engineered cells is changed from 9.4 log cfu per 500 mg to 8.2 log cfu per 500 mg. In summary, these results indicate that the interface around *L. acidophilus* cells has a selectively impermeability to large-scale enzyme molecules that could cause proteolysis of *L. acidophilus* cells and can enhance the stability of cells under gastric and intestinal pH conditions.

In another work, the LbL approach of self-assembly of chitosan and alginate was also used to form a protective interface on the probiotic *Bacillus coagulans* (*B. coagulans*) *via* an

electrostatic adsorption strategy (Fig. 11B(a)).[61] Interestingly, after the interface engineering, the bright field images show that, compared with the native *B. coagulans* cells, the LbL engineered *B. coagulans* cells show aggregation (Fig. 11B(b)i and ii). SEM images show that after the interface engineering, compared with the native cells, there are no significant changes in cell morphology, likely due to the natural polysaccharides in the cell wall of Gram-positive bacteria cells (Fig. 11B(b)iii and iv). This work explores the protective effects of different LbL-engineered interfaces for *B. coagulans* cells against acid (SGF) and bile-salt insults. As we can see from Fig. 11B(c), compared with cells engineered with a single layer of chitosan (*B. coagulans*/$(CHI)_1$), cells engineered with a single bilayer of chitosan and alginate (*B. coagulans*/$(CHI/ALG)_1$ cells) provide a certain protective effect, with a 4 log reduction in CFU against SGF and bile salts. Furthermore, cells engineered with a double bilayer of chitosan and alginate (*B. coagulans*/$(CHI/ALG)_2$ cells) demonstrate significant survival advantages, and just have 1 log reduction in CFU against SGF conditions after 2 h, and a 2 log reduction in CFU against 4% bile salts after 2 h (Fig. 11B(c)). Most importantly, the role of cell-interface engineering in survival and delivery of probiotics *in vivo* is determined by delivering native *B. coagulans* and *B. coagulans*/$(CHI/ALG)_2$ cells by oral gavage. *B. coagulans*/$(CHI/ALG)_2$ cells show an over 6 fold enhanced bioluminescence signal compared to native cells in the background of GI tract, at only 1 h after administration (Fig. 11B(d)).

In addition, a coacervate, composed of cytocompatible cationized protein (bovine serum albumin: BSA-NH_2) and anionized polysaccharides (Dextran-COOH), was designed to construct a protective interface as an artificial cell wall around *Saccharomyces cerevisiae* (*S. cerevisiae*) cells *via* a direct *in situ* self-assembly method (Fig. 11C(a), top).[141] After the cell-surface engineering, the TEM and SEM images confirmed a structurally intact composite biolayer, which firmly adheres to the surface of the cells (Fig. 11C(a), bottom). Due to the α-D-mannose recognition area on the cilia surface of *E. coli*, the native *S. cerevisiae* cells can aggregate within a few minutes *via* a co-culture with *E. coli* cells. But with the artificial interface, there is no clear aggregation, attributed to the protective interface between the *E. coli* and *S. cerevisiae* cells, which blocks the direct contact between them (Fig. 11C(b), top). Moreover, compared with the native cells, the biointerface-engineered cells display a high dye adsorption efficiency; over 70% of the dye could be easily captured within 10 s (Fig. 11C(b), bottom). Surprisingly, the fluorescence images demonstrate that during the fission of the engineered cells, the green and red fluorescence is found on the daughter cells, which suggests that this biointerface around the cells is soft and flexible with a good self-healing performance (Fig. 11C(c)).

In addition to directly engineering living cells with natural saccharides, artificial oligosaccharides containing unusual functional groups can also be introduced on the surface of biological cells *via* metabolic labelling approaches for engineering cell surfaces with special functions, which is considered as an important process in biorthogonal chemistry.[142] This artificial-oligosaccharide-based strategy can incorporate the customized reaction into biological processes within the biological system without affecting normal biochemical processes, which can induce specific modifications for cells in living systems.[143] The unusual specific groups of those cell-surface artificial oligosaccharides can be easily post-modified with versatile materials using efficient, simple, reliable and biocompatible click chemistry to realize cell-surface engineering. For example, Bertozzi and coworkers first proposed a metabolic labelling approach to treat mammalian cells (Jurkat, HL-60, and HeLa cells) with synthesized *N*-levulinoylmannosamine (ManLev) to introduce sialic acid with ketone groups on the cell surface. This can be cell-surface engineered *via* special covalent ligation with molecules containing hydrazide or other complementary reactive functional groups.[144] Moreover, Bertozzi and coworkers developed a strategy to introduce artificial sialic acid with azido groups onto Jurkat cell surfaces by incubating them with *N*-azidoacetylmannosamine (Ac_4ManNAz) (Fig. 12A(a)).[145] Various biological probes or materials with carboxylic acid can be attached to cells based on the cell surface artificial azido groups (Fig. 12A(b)). These chemoselective reactions based on cell-surface artificial azido groups can be conducted according to the requirements of the design, with no reactions from nonspecific amine acylation (Fig. 12A(c)). This metabolic oligosaccharide engineering strategy can label unnatural sugars into cellular glycans for inducing abiotic functionality on the cell surface. Most importantly, this strategy can also be executed for specific labeling in living mice by daily intraperitoneal administration of Ac_4ManNAz for 7 days, after which isolated splenocytes express azido glycans on the surface,[146] which can be quantified with a special phosphine probe with a Flag peptide (Phos-Flag) *via* the Staudinger ligation (Fig. 12B(a)). After treatment with an anti-Flag antibody labeled with isothiocyanate, flow-cytometry analysis shows that the fluorescence of those isolated splenocytes with artificial azido glycans displays a dose-dependent increase (Fig. 12B(b)). Besides that, Zebrafish embryos can also be metabolically labeled with azides on the glycans of their cell surfaces by treatment with *N*-azidoacetylgalactosamine (Ac_4GalNAz) to obtain a novel way to efficiently visualize and probe biomolecules in living systems (Fig. 12C(a)).[147] After a copper-free click chemistry reaction with a fluorophore, those azido glycans of the zebrafish embryos can be stably visualized in a timely way at a subcellular resolution during their development *in vivo* (Fig. 12C(b)), which can provide a reliable spatiotemporal analysis of cell-surface glycan expression and trafficking of zebrafish embryos. As one type of glycosyltransferase isoenzyme, the *N*-acetylgalactosaminyl (GalNAc) transferase family (GalNAc-Ts) can also be used for generating unusual glycans with azido groups on living cell surfaces, which provides a way to probe cell-surface glycosylation (Fig. 12D(a)).[148] Fluorescence images confirmed that the GalNAc-Ts co-localized with the Golgi compartment in cells, which means that the glycosylation is realized here and then transferred and relocated to the surface of the cell membrane (Fig. 12D(b)). Besides that, many synthetic glycopolymers with glycan structures have been designed to insert into cell membranes or to be used for cell-surface engineering.[149,150] This

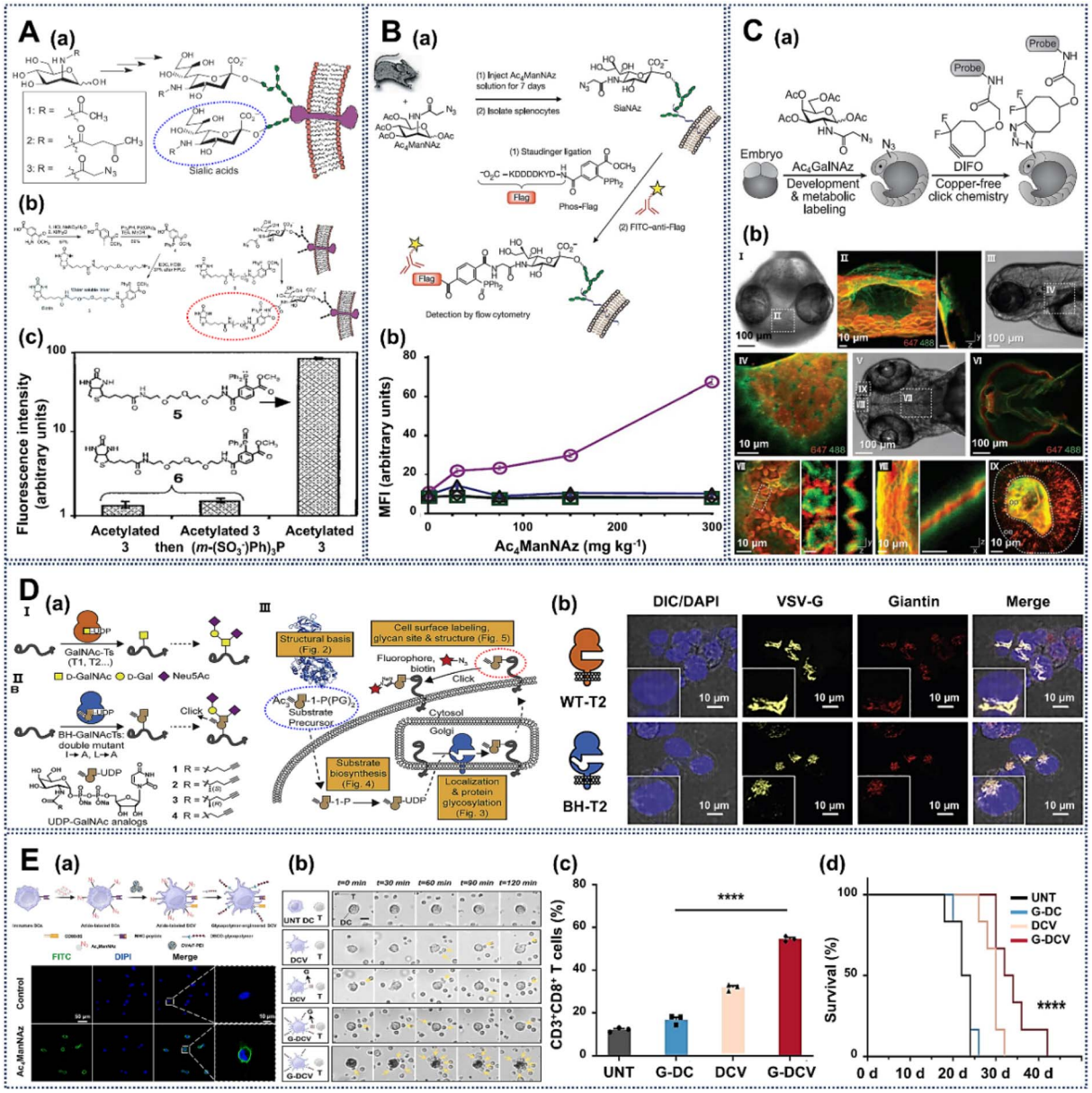

Fig. 12 Creation of engineered cell interfaces based on Jurkat cell-surface artificial oligosaccharides. (A) (a) Metabolic delivery of artificial azido sialic acid to Jurkat cell surfaces with $Ac_4ManNAz$. (b) Reaction of biotinylated phosphine and azides of artificial sialic acid on cell surfaces. (c) Specificity of the Staudinger reaction based on cell-surface unnatural azido sialic acid. Reprinted with permission from ref. 145. Copyright 2000, American Association for the Advancement of Science. (B) (a) The Staudinger ligation and metabolic oligosaccharide engineering with Ac_4-ManNAz *in vivo* in mice. (b) Mean fluorescence intensity (MFI) of the cells treated with different azido-sugar doses. Reprinted with permission from ref. 146. Copyright 2004, Springer Nature. (C) (a) The schematic of the metabolic labeling with $Ac_4GalNAz$ and click chemistry with a fluorescent probe for zebrafish *in vivo*. (b) Identification of temporally distinct artificial glycans during zebrafish development using fluorescence labeling. Reprinted with permission from ref. 147. Copyright 2008, American Association for the Advancement of Science. (D) (a) Schematic of the non-natural-substrate biosynthetic strategy of incorporating chemically tagged sugars onto the cell surface through engineered GalNAc-T glycosyl transferases. (b) Fluorescence images of HepG2 cells transfected with T2 constructs. Reprinted with permission from ref. 148. Copyright 2020, Elsevier. (E) (a) Schematic of preparation of glycopolymer-engineered dendritic cell vaccines (G-DCV) and confocal images of DC labeling with glycopolymer-DBCO after treatment with $Ac_4ManNAz$. (b) The adhesion behavior between G-DCV and T cells. (c) The percentage of $CD^{3+}CD^{8+}$ T cells with or without G-DCV cells. (d) Survival rates of B16-OVA tumor-bearing mice with different treatments. Reprinted with permission from ref. 37. Copyright 2024, Wiley-VCH.

metabolic oligosaccharide-based biorthogonal chemistry strategy provides stable and specific active sites and is recognized as an ideal biotechnology to create engineered cells with customized functions, which has created opportunities for fluorescent labeling, fluorescent probes, manipulation of cell behavior, accurate diagnosis and targeted therapy.[151–153]

Due to their powerful ability to stimulate tumor specific immune responses, dendritic cell vaccines (DCVs) have been

widely used in tumor immunotherapy. Recently, Chen with coworkers developed a glycopolymer-engineered DCV (G-DCV), which has a great potency in antitumor immunotherapy.[37] G-DCV was designed based on stable covalent copper-free click-chemistry between glycopolymers with dibenzocyclooctyne (DBCO) terminal groups and azido-labeled DCs, which were obtained by incubating bone-marrow-derived dendritic cells (BMDCs) with $Ac_4ManNAz$ for 3 days (Fig. 12E(a)).[37] CLSM images show that the glycopolymers with fluorescent monomers can provide a stable and prolonged modification of DCs over 48 hours, which can efficiently induce T-cell activation for immunotherapy. Besides that, compared to native DCs, G-DCs have significantly more T cells adhered (Fig. 12E(b)). Moreover, flow cytometry analysis demonstrates that G-DCV allows stimulation of more $CD8^+$ T cell expansion (Fig. 12E(c)). Notably, G-DCV has a good antitumor effect in a mouse B16-OVA tumor model and significantly prolongs the survival time of B16-OVA mice (Fig. 12E(d)).

Besides these natural molecules, polymers introduced *via* artificially initiated synthesis also represent a powerful means of directly engineering living cell surfaces under mild and biocompatible conditions. They can be called semi-natural molecules, which occupy the space between synthetic polymers and natural biomolecules. Due to the customized polymer synthesis process, this semi-natural polymer-based cell-surface engineering strategy always has good tunability, biocompatibility and precise functions. Unlike traditional cell-surface modification techniques, which often rely on pre-synthesized polymers or chemical conjugation, this strategy allows a controllable and localizable synthesis of polymers directly on cell surfaces. These polymers, synthesized directly on cell surfaces, combine the adaptability of synthetic polymers with the seamless compatibility of biological systems, paving the way for innovations in regenerative medicine, drug delivery, and cell therapy. For example, Hawker and coworkers have introduced an advanced method to engineer live cell surfaces based on polymers *via* artificially initiated synthesis.[58] In this process, cells were treated with activated dibenzocyclooctyl ester to introduce a chain-transfer agent (CTA) onto the cell surfaces, which can provide the active sites to *in situ* graft synthetic polymers through controlled radical polymerization (CRP). The CLSM images demonstrate a stable, uniform shell on the cell surface, confirming the effectiveness of this technique for functionalizing cell surfaces (Fig. 13A(a)).[58] Unlike traditional pre-synthesis methods, this self-synthesizing grafting-from approach initiates polymerization directly on cell surfaces, significantly enhancing grafting efficiency and preserving high cell viability; thus the growth curve of cells functionalized with the semi-natural polymer shows no difference in comparison to those of control groups (Fig. 13A(b)). Besides that, native yeast cells modified with these semi-natural polymers exhibit controlled aggregation in the presence of

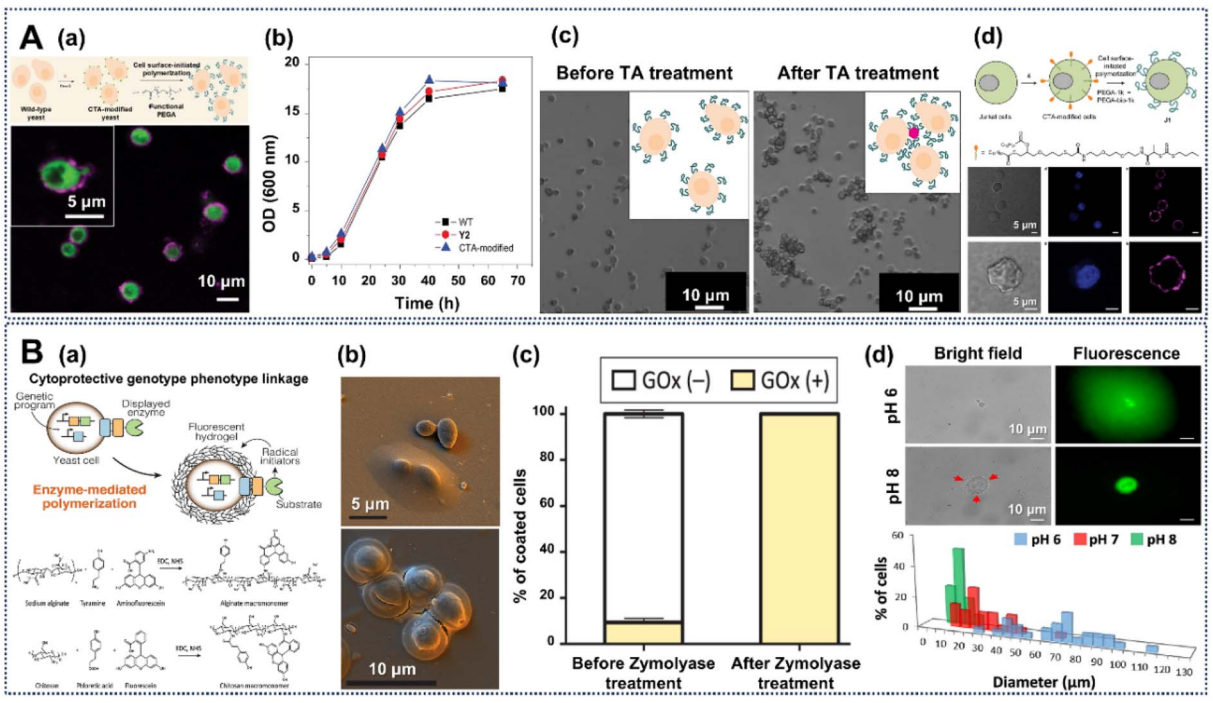

Fig. 13 Creation of engineered cell interfaces based on cell-surface synthesized polymers. (A) (a) Schematic representation of yeast cells modified with surface-initiated photoinduced electron transfer–reversible addition fragmentation chain-transfer polymerization (PET-RAFT) and CLSM images of polymer-modified yeast cells. (b) Growth curves of yeast cells with or without engineering. (c) Bright-field microscope images of engineered yeast cells before and after TA treatment. (d) The surface-initiated PET-RAFT strategy used for engineering Jurkat cells, and the CLSM images of engineered Jurkat cells. Reprinted with permission from ref. 58. Copyright 2017, Springer Nature. (B) (a) Schematic illustration of cell-surface enzyme-mediated polymerization used for engineering yeast cells. (b) SEM images of yeast cells with or without the cell-surface polymerization. (c) Resistance of the encapsulated yeast cells to enzymatic degradation. (d) pH-responsive cell-surface polymerization on cell surface. Reprinted with permission from ref. 154. Copyright 2019, American Chemical Society.

tannic acid (TA), highlighting the ability of the polymer coating to modulate cell behavior (Fig. 13A(c)). Furthermore, this strategy can also be used for mammalian cells, like Jurkat cells, confirming the adaptability and potential for broader biomedical applications, particularly where hybrid synthesis offers combined advantages of biocompatibility and customizable synthetic properties (Fig. 13A(d)).

Moreover, Nash and coworkers developed a cell-surface enzyme-mediated polymer synthesis strategy to build a pH stimuli-responsive hydrogel capsule onto living cells, wherein the capsule is formed by cross-linking phenol-modified alginate and chitosan (Fig. 13B(a)).[154] In the encapsulation process, SEM images show that engineered cells are covered by a smooth, uniform hydrogel layer (Fig. 13B(b)). Importantly, this strategy can selectively engineer living cells expressing glucose oxidase (GOx positive cells), a typical flavin adenine dinucleotide (FAD)-dependent oxidoreductase, and the enzyme-mediated polymerization is based on the enzymatic cascade of glucose oxidase (GOx) and horseradish peroxidase (HRP). When a heterogeneous population of 90% GOx-negative and 10% GOx-positive yeast cells is incubated with zymolyase for 1 h, only GOx-positive cells can survive, which confirmed the selective engineering by this strategy and the resistance of the cell-surface hydrogel capsules to cytotoxic agents (Fig. 13B(c)). Additionally, the cell-surface hydrogel capsules have a pH-responsive property from pH 6 to 8, which can be controlled by adjusting the pH value (Fig. 13B(d)). This adaptability emphasizes the dynamic nature of the synthetic material when combined with natural cellular processes, and underscores the potential of cell-driven synthesis approaches in developing polymers that integrate seamlessly with biological systems.

Similarly, Bruns *et al.* genetically modified yeast cells to express horseradish peroxidase (HRP) on their cell walls, which can drive the cell-surface localized polymerization of various monomers (Fig. 14A(a)).[155] For the *in situ* cell-surface polymerization, grafting-from polymerization was conducted by conjugating a CTA for RAFT polymerization or an alkyl halide atom transfer radical polymerization (ATRP) initiator. After the cell-surface polymerization, the growth curve of PEGMA-engineered Yeast cells by ATRP shows a slower cell division rate due to the stable polymer nanoshell around cells, which limits nutrient uptake and cell expansion (Fig. 14A(b)). The cell-surface PEGMA-based nanoshell also has good resistance to zymolyase digestion (Fig. 14A(c)). Furthermore, based on the azide-group-bearing PEGMA nanoshell on yeast cells, those engineered cells can be quickly and gently labeled with a clickable fluorescent dye (Cy5-DBCO) on the cell surface using click chemistry. CLSM images demonstrate a bright, stable fluorescence localized around cells (Fig. 14A(d)).

Yang *et al.* provide a visible-light-activated graft polymerization of poly(ethylene glycol) diacrylate (PEGDA) as a strategy to engineer yeast cells with a cross-linked nanoshell, which was initiated by cell-surface adsorbed polyethyleneimine (PEI) (Fig. 14B(a)).[156] TEM images confirmed the effective engineering of yeast cells with the poly(PEGDA) nanoshell through the visible-light-induced graft polymerization on the cell surface,

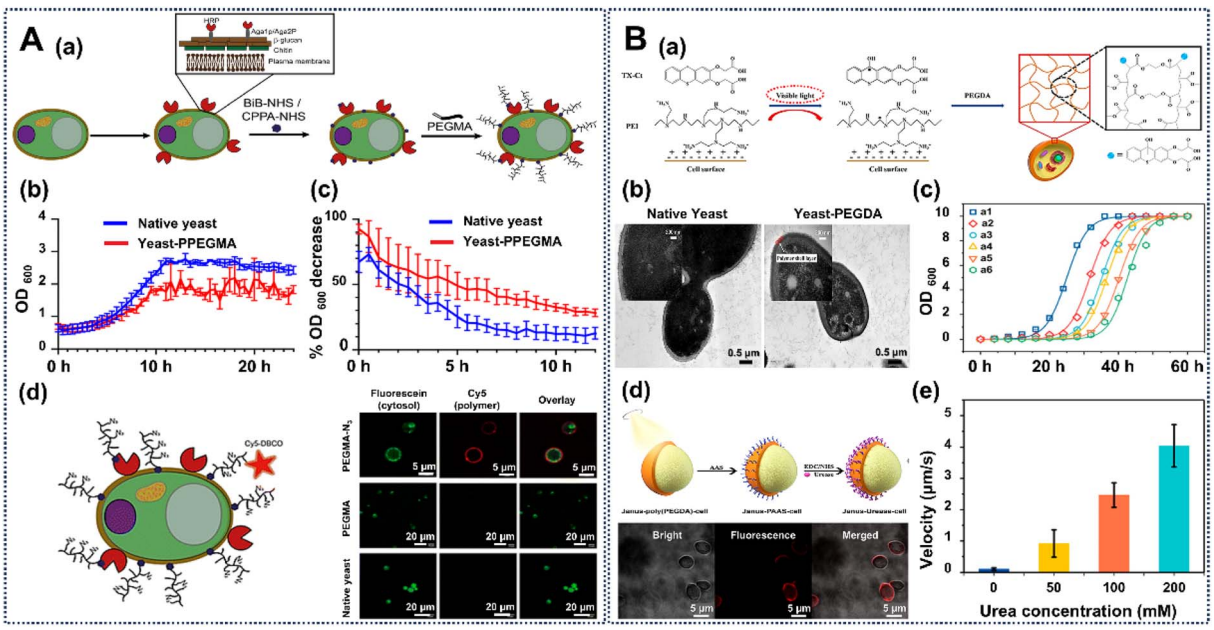

Fig. 14 Creation of engineered cell interfaces based on cell-surface synthesized polymers. (A) (a) Schematic illustration of a horseradish peroxidase (HRP)-catalyzed, grafting-from method on yeast cell surfaces. Growth curve (b) and resistance to zymolyase (c) of native and PPEGMA-engineered yeast cells. (d) Schematic representation of Cy5 conjugation to PPEGMA-N_3 on the cell surface, and CLSM images of Cy5-labeled yeast cells. Reprinted with permission from ref. 155. Copyright 2023, Royal Society of Chemistry. (B) (a) Schematic representation of visible-light-initiated radical graft polymerization of poly(PEGDA) to engineer yeast cells. (b) TEM images of native yeast and yeast-poly(PEGDA) cells. (c) Growth curves of yeast cells with different treatments. (d) Schematic illustration of the preparation process for Janus-Urease cells (top) and CLSM images (bottom) of those cells. (e) The velocity of Janus-Urease cells in urea solutions. Reprinted with permission from ref. 156. Copyright 2021, American Chemical Society.

and indicated that the PEGDA-engineered yeast cells have an about 50 nm polymer nanoshell around them (Fig. 14B(b)). Light-dependent introduction of a cross-linked PEGDA nanoshell around cells can delay cell division due to the suppression of cells' biochemical activity brought about by restricting the transmission of nutrients (Fig. 14B(c)). This means that the integrity and thickness of the polymer nanoshell synthesized on the cell surface can be controlled by adjusting the radiation time and intensity, thereby better manipulating cell behavior. Moreover, the poly(PEGDA) nanoshell around yeast cells can be used as a platform for secondary graft polymerization of sodium acrylate (AAS), which can be performed to modify half of the cell sphere with urease (called a Janus-Urease cell) (Fig. 14B(d)). The Janus-Urease cells exhibited good directional motion through self-propulsion by the cell-surface localized catalytic reactions in urea solutions, which can achieve a concentration gradient velocity control. The velocities of the Janus-Urease cells increase with the increase in urea concentration and can reach 4.04 μm s^{-1} in 200 mmol L^{-1} urea solution, while no obvious motion of the Janus-Urease cell was observed in the absence of urea (Fig. 14B(e)). The use of customized *in situ* semi-natural polymerization for cell-interface engineering represents a versatile and efficient approach to modifying cell surfaces. This technique combines the adaptability of synthetic polymers with the seamless compatibility of biological systems, opening new avenues for innovations in cell therapy, synthetic biology, and biocatalysis.

3. Remaining challenges

As an interdisciplinary scientific field with biology, physics, chemistry, materials science and engineering science, aimed at redesigning and constructing living-cell–material hybrid biological systems with new functions, cell-interface engineering technology has developed into a global topic, and has had a profound impact on multiple fields such as biomedicine, agriculture, industrial production, and even energy conversion. The development of science and bio/nanotechnology has made significant research progress in the field of customized synthetic cell-interface engineering. These studies not only advance our understanding of the essence of matter and life, but also open new paths for future technological development. As shown in Fig. 15, there are still some challenges that urgently need to be addressed:

(1) Novel biointerfaces with precise controllability and functionality on the cell surface. This requires selecting suitable molecular components of materials and designing appropriate assembly mechanisms to construct interfaces with automatic assembly of fine structures and functions on the cell surface to achieve functional integration. This would ensure that engineered cells can perform specific functions (such as molecular transfer, or various biochemical triggers), thereby improving the functionality and stability of engineered cells.

(2) How to design self-sustaining and self-regenerating biological interfaces around cells. The stability of cell-surface nanocoatings brought about by current cell-surface engineering technology may disappear with cell proliferation, along with the functionality provided by the interface to the living cells. Finding how to develop a self-sustaining and self-healing interface structures around cells requires further advances in materials and synthesis methods, which can ensure that a cell-surface nanoshell can respond to environmental changes for self-healing and morphological changes, thereby maintaining the long-term stability of engineered cells.

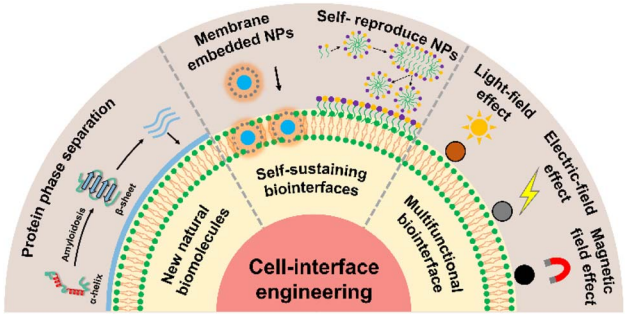

Fig. 15 The challenges and future research outlook of next-generation cell-interface engineering systems.

(3) Enlarging the application scope for engineered cells. The functionality of the currently developed engineering cells is relatively focussed, and expanding the application scope of engineered cells will help promote the development of cell engineering research. Utilizing cell engineering technology to achieve efficient utilization of resources and sustainable management of the environment could promote the development of society towards a greener and more sustainable direction.

4. Future outlook

Cell-interface engineering using biomolecules has made significant progress and has wide applications in biotechnology.[157–161] In order to promote the wider application and development of natural-molecule-based cell-interface engineering, sustained progress is ongoing in the design and improvement of these hybrid systems.[162–166] We have raised the goals listed below as some of those that ought to be addressed in future studies within the field of cell-interface engineering (Fig. 15).

(1) Developing new natural biomolecules to expand multi-function cell-interface engineering. Natural biomolecules have a unique advantage of biocompatibility, compared to other materials. Aside from the comparison with other materials, more biomolecules with special properties in living processes should be applied in cell-interface engineering. In one of the main pathological features of Alzheimer's disease, the amyloid-β peptide obtained by hydrolysis of amyloid precursor proteins can cause plaques, which possess a strong aggregation potential.[167] In this case, amyloidosis occurs to transform three-dimensional proteins into planar peptides with the stable conformation of a β-pleated sheet lamellar structure and exposes more active binding sites. Inspired by this phenomenon, phase-transformed proteins are good candidates to

construct a universal biointerface on living cell surfaces and induce nanomaterial assembly.

(2) Developing a new generation of biointerfaces around cells for efficient applications. Most efforts have focused on the construction of extracellular biointerfaces up to now. However, proliferation, a natural property of living cells, is an uncontrollable process, and would destroy the interface during the process or be inhibited by the rigid interface, affecting cell functions. Therefore, a new-generation design of intracellular biointerfaces around cells is most desired. Cell membrane-embedded interfaces have great potential in intracellular biointerface design.[168,169] By embedding biomolecules into the cell membrane, the exogenous interface is most closely combined with cells to obtain a real sense of an artificial cell membrane for "living" functions. This new type of biointerface would minimize the impact on or by cells. Furthermore, to address the challenge of the disappearance of engineered cell-surface nanoshells and their functions caused by cell proliferation, it is necessary to select self-reproducing molecules and construct a self-sustaining nanoshell on cell surfaces.[170] Thus, nanoshells on the surface of cells would have a self-reproducing effect with cell proliferation to maintain the stability of the nanoshell functions around cells, thereby obtaining true "living materials".

(3) Developing engineered cells with integrated multiple functions to expand the applications of engineered cell-based biological systems. For example, Brinker *et al.* simultaneously introduced multiple functional materials onto the surface of HeLa cells, which provides the potential to introduce multiple functionalities for different applications.[81] In addition, by coupling the effects of multiple physical fields, such as light, electrical and magnetic fields, materials can be utilized to activate and promote the application of engineered cells. For example, the use of electric-field stimulation can significantly enhance the hydrogen production performance of living cells.[97]

5. Conclusion

In this review, we introduce cell-interface engineering with functional materials based on natural biomolecules. These molecules include rich functional groups with great biocompatibility, and thus have been applied by researchers in recent years. We have mainly reviewed the history and the progress of 5 types of natural biomolecule (*i.e.*, DNA polymers, amino acids, polyphenols, proteins and polysaccharides) that can be effectively integrated into cell interfaces. We explore challenges and prospects in the field of cell-interface engineering. We believe that our work will play a role in guiding next-generation cell-interface engineering, as well as better utilizing and manipulating cells, thereby creating new opportunities for the development of cell-based biotechnologies in the future.

Data availability

No primary research results, software or code have been included and no new data were generated or analysed as part of this review. Data available on request from the authors.

Author contributions

Conceptualization: X. Y. Yang, Y. Q. Huang, W. Geng and T. K. Zhang; writing the original draft: T. K. Zhang, Z. Q. Yi and Y. Q. Huang; validation: T. K. Zhang, Z. Q. Yi and Y. Q. Huang; review and editing: X. Y. Yang, Y. Q. Huang and W. Geng.

Conflicts of interest

The authors declare no conflict of interest.

Acknowledgements

This study is supported by the National Key Research and Development Program of China (2022YFB3805600, 2022YFB3805604), National Natural Science Foundation of China (22293020), Major Program (JD) of Hubei Province (2023BAA003), Key R&D Program of Shandong Province, China (2023CXGC010314), Technology Innovation Program of Hubei Province (2023BIB018) and National 111 project (B20002).

References

1 M. Lynch, M. C. Field, H. V. Goodson, H. S. Malik, J. B. Pereira-Leal, D. S. Roos, A. P. Turkewitz and S. Sazer, *Proc. Natl. Acad. Sci. U. S. A.*, 2014, **111**, 16990–16994.
2 D. Arendt, J. M. Musser, C. V. H. Baker, A. Bergman, C. Cepko, D. H. Erwin, M. Pavlicev, G. Schlosser, S. Widder, M. D. Laubichler and G. P. Wagner, *Nat. Rev. Genet.*, 2016, **17**, 744–757.
3 Z. Guo, J. Richardson, B. Kong and K. Liang, *Sci. Adv.*, 2020, **6**, eaaz0330.
4 J. Sun, L. Gao, L. Wang and X. Sun, *Talanta*, 2021, **234**, 122671.
5 W. L. Nicholson, N. Munakata, G. Horneck, H. J. Melosh and P. Setlow, *Microbiol. Mol. Biol. Rev.*, 2000, **64**, 548–572.
6 P. Setlow, *Bacterial Stress Responses*, ed. G. Storz and R. Hengge, ASM Press, Washington, 2nd edn, 2010, pp. 319–332.
7 J. Errington, *Nat. Rev. Microbiol.*, 2003, **1**, 117–126.
8 L. Addadi, D. Joester, F. Nudelman and S. Weiner, *Chem.–Eur. J.*, 2006, **12**, 980–987.
9 J. Prywer, *Science*, 2022, **376**, 240–241.
10 L. Wang, Y. Li, X.-Y. Yang, B.-B. Zhang, N. Ninane, H. J. Busscher, Z.-Y. Hu, C. Delneuville, N. Jiang, H. Xie, G. Van Tendeloo, T. Hasan and B.-L. Su, *Natl. Sci. Rev.*, 2021, **8**, nwaa097.
11 S. Zheng, J. Shen, Y. Jiao, Y. Liu, C. Zhang, M. Wei, S. Hao and X. Zeng, *Cancer Sci.*, 2009, **100**, 859–865.
12 B. Ma and A. Bianco, *Nat. Rev. Mater.*, 2023, **8**, 403–413.
13 H. Yang, L. Yao, Y. Wang, G. Chen and H. Chen, *Chem. Sci.*, 2023, **14**, 13325–13345.
14 Y. Wang, Z. Li, F. Mo, T. J. Chen-Mayfield, A. Saini, A. M. LaMere and Q. Hu, *Chem. Soc. Rev.*, 2023, **52**, 1068–1102.
15 S. Yao, B. Jin, Z. Liu, C. Shao, R. Zhao, X. Wang and R. Tang, *Adv. Mater.*, 2017, **29**, 1605903.

16 W. Geng, L. Wang, N. Jiang, J. Cao, Y. X. Xiao, H. Wei, A. K. Yetisen, X. Y. Yang and B. L. Su, *Nanoscale*, 2018, **10**, 3112–3129.
17 Q. W. Chen, J. Y. Qiao, X. H. Liu, C. Zhang and X. Z. Zhang, *Chem. Soc. Rev.*, 2021, **50**, 12576–12615.
18 H. Lee, N. Kim, H. B. Rheem, B. J. Kim, J. H. Park and I. S. Choi, *Adv. Healthcare Mater.*, 2021, **10**, e2100347.
19 T.-K. Zhang, W. Geng, Y.-Q. Huang, F.-Z. Wang, G. Tian and X.-Y. Yang, *Coord. Chem. Rev.*, 2024, **498**, 215471.
20 Z. C. Lu, R. Zhang, H. Z. Liu, J. X. Zhou and H. F. Su, *Trends Biotechnol.*, 2024, **42**, 91–103.
21 H. X. Han, L. J. Tian, D. F. Liu, H. Q. Yu, G. P. Sheng and Y. Xiong, *J. Am. Chem. Soc.*, 2022, **144**, 6434–6441.
22 B. Wang, C. Zeng, K. H. Chu, D. Wu, H. Y. Yip, L. Ye and P. K. Wong, *Adv. Energy Mater.*, 2017, **7**, 1700611.
23 Y. Honda, H. Hagiwara, S. Ida and T. Ishihara, *Angew. Chem., Int. Ed.*, 2016, **55**, 8045–8048.
24 Z. Xu, J. Qi, S. Wang, X. Liu, M. Li, S. Mann and X. Huang, *Nat. Commun.*, 2023, **14**, 1872.
25 B. Cao, Z. Zhao, L. Peng, H.-Y. Shiu, M. Ding, F. Song, X. Guan, C. K. Lee, J. Huang, D. Zhu, X. Fu, G. C. L. Wong, C. Liu, K. Nealson, P. S. Weiss, X. Duan and Y. Huang, *Science*, 2021, **373**, 1336–1340.
26 H. Zhang, H. Liu, Z. Tian, D. Lu, Y. Yu, S. Cestellos-Blanco, K. K. Sakimoto and P. Yang, *Nat. Nanotechnol.*, 2018, **13**, 900–905.
27 J. Guo, M. Suástegui, K. Sakimoto Kelsey, M. Moody Vanessa, G. Xiao, G. Nocera Daniel and S. Joshi Neel, *Science*, 2018, **362**, 813–816.
28 K. Sakimoto, A. Wong and P. Yang, *Science*, 2016, **351**, 74–77.
29 L. Qin, M. Gao, M. Zhang, L. Feng, Q. Liu and G. Zhang, *Water Res.*, 2020, **187**, 116430.
30 H. Qin, T. Hu, Y. Zhai, N. Lu and J. Aliyeva, *J. Hazard. Mater.*, 2020, **400**, 123161.
31 H. Hu, X. Liang, S. Wang, Z. Xu, J. Li, H. Chen, D. Su, Y. Yin, Z. Huang and X. Huang, *Macromol. Biosci.*, 2020, **20**, e2000185.
32 Y. Jia, Y. Chen and Y. Hu, *ACS ES&T Water*, 2021, **1**, 2412–2422.
33 F. Cao, L. Jin, Y. Gao, Y. Ding, H. Wen, Z. Qian, C. Zhang, L. Hong, H. Yang, J. Zhang, Z. Tong, W. Wang, X. Chen and Z. Mao, *Nat. Nanotechnol.*, 2023, **18**, 617–627.
34 F. Zhang, J. Zhuang, Z. Li, H. Gong, B. E. de Avila, Y. Duan, Q. Zhang, J. Zhou, L. Yin, E. Karshalev, W. Gao, V. Nizet, R. H. Fang, L. Zhang and J. Wang, *Nat. Mater.*, 2022, **21**, 1324–1332.
35 R. Sun, M. Liu, J. Lu, B. Chu, Y. Yang, B. Song, H. Wang and Y. He, *Nat. Commun.*, 2022, **13**, 5127.
36 C. Sigl, E. M. Willner, W. Engelen, J. A. Kretzmann, K. Sachenbacher, A. Liedl, F. Kolbe, F. Wilsch, S. A. Aghvami, U. Protzer, M. F. Hagan, S. Fraden and H. Dietz, *Nat. Mater.*, 2021, **20**, 1281–1289.
37 H. Yang, Z. Xiong, X. Heng, X. Niu, Y. Wang, L. Yao, L. Sun, Z. Liu and H. Chen, *Angew. Chem., Int. Ed.*, 2024, **63**, e202315782.
38 H. Wei, X.-Y. Yang, W. Geng, H. C. van der Mei and H. J. Busscher, *Nanoscale*, 2021, **13**, 7220–7233.
39 J. Park, B. Andrade, Y. Seo, M.-J. Kim, S. C. Zimmerman and H. Kong, *Chem. Rev.*, 2018, **118**, 1664–1690.
40 J. Almeida-Pinto, M. R. Lagarto, P. Lavrador, J. F. Mano and V. M. Gaspar, *Adv. Sci.*, 2023, **10**, 2304040.
41 S. Yang, H. Choi, D. T. Nguyen, N. Kim, S. Y. Rhee, S. Y. Han, H. Lee and I. S. Choi, *Adv. Ther.*, 2023, **6**, 2300037.
42 W. Geng, N. Jiang, G. Y. Qing, X. Liu, L. Wang, H. J. Busscher, G. Tian, T. Sun, L. Y. Wang, Y. Montelongo, C. Janiak, G. Zhang, X. Y. Yang and B. L. Su, *ACS Nano*, 2019, **13**, 14459–14467.
43 W. Youn, E. H. Ko, M. H. Kim, M. Park, D. Hong, G. A. Seisenbaeva, V. G. Kessler and I. S. Choi, *Angew. Chem., Int. Ed.*, 2017, **56**, 10702–10706.
44 W. Li, Z. Liu, C. Liu, Y. Guan, J. Ren and X. Qu, *Angew. Chem., Int. Ed.*, 2017, **56**, 13661–13665.
45 P. Zhang, C. Yang, Z. Li, J. Liu, X. Xiao, D. Li, C. Chen, M. Yu and Y. Feng, *Electrochim. Acta*, 2022, **421**, 140490.
46 A. Yulaev, A. Lipatov, A. X. Lu, A. Sinitskii, M. S. Leite and A. Kolmakov, *Adv. Mater. Interfaces*, 2017, **4**, 1600734.
47 R. Kempaiah, A. Chung and V. Maheshwari, *ACS Nano*, 2011, **5**, 6025–6031.
48 H. Di, H. Liu, M. Li, J. Li and D. Liu, *Anal. Chem.*, 2017, **89**, 5874–5881.
49 V. Maheshwari, D. E. Fomenko, G. Singh and R. F. Saraf, *Langmuir*, 2010, **26**, 371–377.
50 T.-K. Zhang, Z.-Q. Yi, K.-Q. Ye, W. Geng, Y.-Q. Huang, G. Tian and X.-Y. Yang, *Chem. Phys. Lett.*, 2023, **829**, 140750.
51 Z. Jiang, Y. Liu, R. Shi, X. Feng, W. Xu, X. Zhuang, J. Ding and X. Chen, *Adv. Mater.*, 2022, **34**, e2110094.
52 N. Tang, H. Li, L. Zhang, X. Zhang, Y. Chen, H. Shou, S. Feng, X. Chen, Y. Luo, R. Tang and B. Wang, *Angew. Chem., Int. Ed.*, 2021, **60**, 6509–6517.
53 C. Chen, H. Zhang, L. Yang, W. Lv, L. Zhang, X. Jiang and D. Sun, *ACS Sustainable Chem.*, 2021, **9**, 9854–9860.
54 L. Yue, K. Yang, X.-Y. Lou, Y.-W. Yang and R. Wang, *Matter*, 2020, **3**, 1557–1588.
55 J. T. Wilson, W. Cui, V. Kozlovskaya, E. Kharlampieva, D. Pan, Z. Qu, V. R. Krishnamurthy, J. Mets, V. Kumar, J. Wen, Y. Song, V. V. Tsukruk and E. L. Chaikof, *J. Am. Chem. Soc.*, 2011, **133**, 7054–7064.
56 J. Liu, Y. Wang, W. J. Heelan, Y. Chen, Z. Li and Q. Hu, *Sci. Adv.*, 2022, **8**, eabp8798.
57 Y. Niu, D. Xue, X. Dai, G. Guo, X. Yang, L. Yang and Z. Bai, *Nat. Sustain.*, 2024, **7**, 1182–1189.
58 J. Niu, D. J. Lunn, A. Pusuluri, J. I. Yoo, M. A. O'Malley, S. Mitragotri, H. T. Soh and C. J. Hawker, *Nat. Chem.*, 2017, **9**, 537–545.
59 L. Wang, Z. Cao, M. Zhang, S. Lin and J. Liu, *Adv. Mater.*, 2022, **34**, e2106669.
60 Z. Zhao, D. C. Pan, Q. M. Qi, J. Kim, N. Kapate, T. Sun, C. W. t. Shields, L. L. Wang, D. Wu, C. J. Kwon, W. He, J. Guo and S. Mitragotri, *Adv. Mater.*, 2020, **32**, e2003492.
61 A. C. Anselmo, K. J. McHugh, J. Webster, R. Langer and A. Jaklenec, *Adv. Mater.*, 2016, **28**, 9486–9490.

62 S. Kaushik, P. D. Thungon and P. Goswami, *ACS Biomater. Sci. Eng.*, 2020, **6**, 4337–4355.
63 P. Auffinger, F. A. Hays, E. Westhof and P. S. Ho, *Proc. Natl. Acad. Sci. U. S. A.*, 2004, **101**, 16789–16794.
64 J. Clardy and C. Walsh, *Nature*, 2004, **432**, 829–837.
65 L. S. Hui Chong, J. Zhang, K. S. Bhat, D. Yong and J. Song, *Biomaterials*, 2021, **266**, 120473.
66 E. Tvrda, F. Benko, T. Slanina and S. S. du Plessis, *Molecules*, 2021, **26**, 5196.
67 Y. Ju, H. Liao, J. J. Richardson, J. Guo and F. Caruso, *Chem. Soc. Rev.*, 2022, **51**, 4287–4336.
68 S. H. Yang, S. M. Kang, K. B. Lee, T. D. Chung, H. Lee and I. S. Choi, *J. Am. Chem. Soc.*, 2011, **133**, 2795–2797.
69 A. J. Priya, S. P. Vijayalakshmi and A. M. Raichur, *J. Agric. Food Chem.*, 2011, **59**, 11838–11845.
70 N. Jiang, G. L. Ying, S. Y. Liu, L. Shen, J. Hu, L. J. Dai, X. Y. Yang, G. Tian and B. L. Su, *Chem. Commun.*, 2014, **50**, 15407–15410.
71 Z. Yi, S. Tian, W. Geng, T. Zhang, W. Zhang, Y. Huang, H.-N. Barad, G. Tian and X.-Y. Yang, *Chem.–Eur. J.*, 2023, **29**, e202203662.
72 K. Adebowale, R. Liao, V. C. Suja, N. Kapate, A. Lu, Y. Gao and S. Mitragotri, *Adv. Mater.*, 2023, 2210059.
73 W. Xiong, Y. Peng, W. Ma, X. Xu, Y. Zhao, J. Wu and R. Tang, *Natl. Sci. Rev.*, 2023, **10**, nwad200.
74 Y. H. Roh, R. C. Ruiz, S. Peng, J. B. Lee and D. Luo, *Chem. Soc. Rev.*, 2011, **40**, 5730–5744.
75 M. R. Jones, N. C. Seeman and C. A. Mirkin, *Science*, 2015, **347**, 1260901.
76 X. Wang, W. E. Allen, M. A. Wright, E. L. Sylwestrak, N. Samusik, S. Vesuna, K. Evans, C. Liu, C. Ramakrishnan, J. Liu, G. P. Nolan, F.-A. Bava and K. Deisseroth, *Science*, 2018, **361**, eaat5691.
77 X. Xiong, H. Liu, Z. Zhao, M. B. Altman, D. Lopez-Colon, C. J. Yang, L. J. Chang, C. Liu and W. Tan, *Angew. Chem., Int. Ed.*, 2013, **52**, 1472–1476.
78 Y. Chen, R. Tian, Y. Shang, Q. Jiang and B. Ding, *Adv. NanoBiomed Res.*, 2022, **2**, 2100126.
79 P. Shi and Y. Wang, *Angew. Chem., Int. Ed.*, 2021, **60**, 11580–11591.
80 Z. J. Gartner and C. R. Bertozzi, *Proc. Natl. Acad. Sci. U. S. A.*, 2009, **106**, 4606–4610.
81 P. Shi, N. Zhao, J. Coyne and Y. Wang, *Nat. Commun.*, 2019, **10**, 2223.
82 T. Gao, T. Chen, C. Feng, X. He, C. Mu, J. I. Anzai and G. Li, *Nat. Commun.*, 2019, **10**, 2946.
83 Y. Hou and G. Wu, *Adv. Nutr.*, 2018, **9**, 849–851.
84 G. Wu, *Amino acids biochemistry and nutrition*, CRC Press, Texas, USA, 2021.
85 T. A. King, J. Mandrup Kandemir, S. J. Walsh and D. R. Spring, *Chem. Soc. Rev.*, 2021, **50**, 39–57.
86 B. Kelly and E. L. Pearce, *Cell Metab.*, 2020, **32**, 154–175.
87 R. P. Wilson, in *Fish Nutrition*, ed. J. E. Halver, R. W. Hardy, Academic Press, San Diego, 3rd edn, 2003, pp. 143–179.
88 A. Meister, *Science*, 1973, **180**, 33–39.
89 N. Jiang, X. Y. Yang, G. L. Ying, L. Shen, J. Liu, W. Geng, L. J. Dai, S. Y. Liu, J. Cao, G. Tian, T. L. Sun, S. P. Li and B. L. Su, *Chem. Sci.*, 2015, **6**, 486–491.
90 N. Jiang, G. L. Ying, A. K. Yetisen, Y. Montelongo, L. Shen, Y. X. Xiao, H. J. Busscher, X. Y. Yang and B. L. Su, *Chem. Sci.*, 2018, **9**, 4730–4735.
91 J. G. Handique and J. B. Baruah, *React. Funct. Polym.*, 2002, **52**, 163–188.
92 D. Wu, J. Zhou, M. N. Creyer, W. Yim, Z. Chen, P. B. Messersmith and J. V. Jokerst, *Chem. Soc. Rev.*, 2021, **50**, 4432–4483.
93 X. Zhang, Z. Li, P. Yang, G. Duan, X. Liu, Z. Gu and Y. Li, *Mater. Horiz.*, 2021, **8**, 145–167.
94 Y. Guo, Q. Sun, F. G. Wu, Y. Dai and X. Chen, *Adv. Mater.*, 2021, **33**, 2007356.
95 J. Zhou, Z. Lin, Y. Ju, M. A. Rahim, J. J. Richardson and F. Caruso, *Acc. Chem. Res.*, 2020, **53**, 1269–1278.
96 W. Zhu, J. Guo, S. Amini, Y. Ju, J. O. Agola, A. Zimpel, J. Shang, A. Noureddine, F. Caruso, S. Wuttke, J. G. Croissant and C. J. Brinker, *Adv. Mater.*, 2019, **31**, 1900545.
97 W. Zhou, W. Zhang, W. Geng, Y. Huang, T. K. Zhang, Z. Q. Yi, Y. Ge, Y. Huang, G. Tian and X. Y. Yang, *ACS Nano*, 2024, **18**, 10840–10849.
98 H. Lee, S. M. Dellatore, W. M. Miller and P. B. Messersmith, *Science*, 2007, **318**, 426–430.
99 C. Pan, J. Li, W. Hou, S. Lin, L. Wang, Y. Pang, Y. Wang and J. Liu, *Adv. Mater.*, 2021, **33**, 2007379.
100 H. Cao, L. Yang, R. Tian, H. Wu, Z. Gu and Y. Li, *Chem. Soc. Rev.*, 2022, **51**, 4175–4198.
101 X. He, E. Obeng, X. Sun, N. Kwon, J. Shen and J. Yoon, *Mater. Today Bio*, 2022, **15**, 100329.
102 Z. Jin, L. Yang, S. Shi, T. Wang, G. Duan, X. Liu and Y. Li, *Adv. Funct. Mater.*, 2021, **31**, 2103391.
103 H. A. Lee, E. Park and H. Lee, *Adv. Mater.*, 2020, **32**, 1907505.
104 B. Wang, G. Wang, B. Zhao, J. Chen, X. Zhang and R. Tang, *Chem. Sci.*, 2014, **5**, 3463–3468.
105 H. Guo, Z. Cao, J. Li, Z. Fu, S. Lin, L. Wang and J. Liu, *ACS Nano*, 2023, **17**, 5059–5071.
106 L. Wang, B.-B. Zhang, X.-Y. Yang and B.-L. Su, *Colloids Surf., B*, 2022, **214**, 112454.
107 Y. Zhao, M. Fan, Y. Chen, Z. Liu, C. Shao, B. Jin, X. Wang, L. Hui, S. Wang, Z. Liao, D. Ling, R. Tang and B. Wang, *Sci. Adv.*, 2020, **6**, eaaw9679.
108 Y. Y. Yu, Y. Z. Wang, Z. Fang, Y. T. Shi, Q. W. Cheng, Y. X. Chen, W. Shi and Y. C. Yong, *Nat. Commun.*, 2020, **11**, 4087.
109 D. Vona, S. R. Cicco, R. Ragni, C. Vicente-Garcia, G. Leone, M. M. Giangregorio, F. Palumbo, E. Altamura and G. M. Farinola, *Photochem. Photobiol. Sci.*, 2022, **21**, 949–958.
110 L. Wang, Z. Y. Hu, X. Y. Yang, B. B. Zhang, W. Geng, G. Van Tendeloo and B. L. Su, *Chem. Commun.*, 2017, **53**, 6617–6620.
111 Y. Liu, M. Zhang, X. Wang, F. Yang, Z. Cao, L. Wang and J. Liu, *Adv. Mater.*, 2023, **35**, 2210949.

112 C. Pan, L. Wang, M. Zhang, J. Li, J. Liu and J. Liu, *J. Am. Chem. Soc.*, 2023, **145**, 13261–13272.
113 Y. Li, Y. Miao, L. Yang, Y. Zhao, K. Wu, Z. Lu, Z. Hu and J. Guo, *Adv. Sci.*, 2022, **9**, 2202684.
114 W. Li, W. Bing, S. Huang, J. Ren and X. Qu, *Adv. Funct. Mater.*, 2015, **25**, 3775–3784.
115 H. Ejima, J. Richardson, K. Liang, J. Best, M. van Koeverden, G. Such, J. Cui and F. Caruso, *Science*, 2013, **341**, 154–157.
116 C. Zhang, X. Gao, X. Ren, T. Xu, Q. Peng, Y. Zhang, Z. Chao, W. Jiang, L. Jia and L. Han, *ACS Nano*, 2023, **17**, 6886–6898.
117 J. Pan, G. Gong, Q. Wang, J. Shang, Y. He, C. Catania, D. Birnbaum, Y. Li, Z. Jia, Y. Zhang, N. S. Joshi and J. Guo, *Nat. Commun.*, 2022, **13**, 2117.
118 B. J. Kim, S. Han, K. B. Lee and I. S. Choi, *Adv. Mater.*, 2017, **29**, 1700784.
119 J. H. Park, K. Kim, J. Lee, J. Y. Choi, D. Hong, S. H. Yang, F. Caruso, Y. Lee and I. S. Choi, *Angew. Chem., Int. Ed.*, 2014, **53**, 12420–12425.
120 G. Fan, P. Wasuwanich, M. R. Rodriguez-Otero and A. L. Furst, *J. Am. Chem. Soc.*, 2022, **144**, 2438–2443.
121 Y. Miyamoto-Shinohara, T. Imaizumi, J. Sukenobe, Y. Murakami, S. Kawamura and Y. Komatsu, *Cryobiology*, 2000, **41**, 251–255.
122 U. T. Bornscheuer, B. Hauer, K. E. Jaeger and U. Schwaneberg, *Angew. Chem., Int. Ed.*, 2019, **58**, 36–40.
123 P. Guo, D. Wang, S. Zhang, D. Cheng, S. Wu, X. Zuo, Y. B. Jiang and T. Jiang, *Nano Lett.*, 2023, **23**, 6386–6392.
124 M. Mahmoudi, M. P. Landry, A. Moore and R. Coreas, *Nat. Rev. Mater.*, 2023, **8**, 422–438.
125 M. J. Harrington and P. Fratzl, *Prog. Mater. Sci.*, 2021, **120**, 100767.
126 Y. Zhang, Y. Liu, Y. Liu, P. Zuo, S. Miao, B. Hu, Y. Kang, W. Liu, Q. Yang, H. Ren and P. Yang, *J. Am. Chem. Soc.*, 2023, **145**, 17125–17135.
127 X. Zhang, C. Long, X. Zhu, X. Zhang, J. Li, J. Luo, J. Li and Q. Gao, *ACS Nano*, 2023, **17**, 18850–18863.
128 I. Drachuk, O. Shchepelina, S. Harbaugh, N. Kelley-Loughnane, M. Stone and V. V. Tsukruk, *Small*, 2013, **9**, 3128–3137.
129 J. Yang, J. Li, X. Li, X. Wang, Y. Yang, N. Kawazoe and G. Chen, *Biomaterials*, 2017, **133**, 253–262.
130 R. Liu, J. Zhao, Q. Han, X. Hu, D. Wang, X. Zhang and P. Yang, *Adv. Mater.*, 2018, **30**, 1802851.
131 A. Matsuzawa, M. Matsusaki and M. Akashi, *Langmuir*, 2013, **29**, 7362–7368.
132 K. Liang, J. J. Richardson, C. J. Doonan, X. Mulet, Y. Ju, J. Cui, F. Caruso and P. Falcaro, *Angew. Chem., Int. Ed.*, 2017, **56**, 8510–8515.
133 J. Liu, L. Shi, Y. Deng, M. Zou, B. Cai, Y. Song, Z. Wang and L. Wang, *Biomaterials*, 2022, **287**, 121638.
134 J. K. Sahoo, O. Hasturk, T. Falcucci and D. L. Kaplan, *Nat. Rev. Chem*, 2023, **7**, 302–318.
135 O. Hasturk, J. K. Sahoo and D. L. Kaplan, *Biomacromolecules*, 2020, **21**, 2829–2843.
136 S. Boddohi and M. J. Kipper, *Adv. Mater.*, 2010, **22**, 2998–3016.
137 S. Mizrahy and D. Peer, *Chem. Soc. Rev.*, 2012, **41**, 2623–2640.
138 J. F. Wardman, R. K. Bains, P. Rahfeld and S. G. Withers, *Nat. Rev. Microbiol.*, 2022, **20**, 542–556.
139 E. Drula, M.-L. Garron, S. Dogan, V. Lombard, B. Henrissat and N. Terrapon, *Nucleic Acids Res.*, 2022, **50**, D571–D577.
140 M. F. Chaplin, *Carbohydrate analysis*, Wiley-VCH, Weinheim, 2006, pp. 243–275.
141 D. Su, X. Liu, L. Liu, L. Wang, H. Xie, H. Zhang, X. Meng and X. Huang, *Adv. Funct. Mater.*, 2018, **28**, 1705699.
142 K. K. Palaniappan and C. R. Bertozzi, *Chem. Rev.*, 2016, **116**, 14277–14306.
143 V. K. Tiwari, M. K. Jaiswal, S. Rajkhowa and S. K. Singh, in *Click Chemistry*, ed. V. K. Tiwari, M. K. Jaiswal, S. Rajkhowa and S. K. Singh, Springer Nature Singapore, Singapore, 2024, pp. 175–203.
144 L. K. Mahal, K. J. Yarema and C. R. Bertozzi, *Science*, 1997, **276**, 1125–1128.
145 E. Saxon and C. R. Bertozzi, *Science*, 2000, **287**, 2007–2010.
146 J. A. Prescher, D. H. Dube and C. R. Bertozzi, *Nature*, 2004, **430**, 873–877.
147 S. T. Laughlin, J. M. Baskin, S. L. Amacher and C. R. Bertozzi, *Science*, 2008, **320**, 664–667.
148 B. Schumann, S. A. Malaker, S. P. Wisnovsky, M. F. Debets, A. J. Agbay, D. Fernandez, L. J. S. Wagner, L. Lin, Z. Li, J. Choi, D. M. Fox, J. Peh, M. A. Gray, K. Pedram, J. J. Kohler, M. Mrksich and C. R. Bertozzi, *Mol. Cell*, 2020, **78**, 824–834.
149 J. R. Kramer, B. Onoa, C. Bustamante and C. R. Bertozzi, *Proc. Natl. Acad. Sci. U. S. A.*, 2015, **112**, 12574–12579.
150 D. Rabuka, M. B. Forstner, J. T. Groves and C. R. Bertozzi, *J. Am. Chem. Soc.*, 2008, **130**, 5947–5953.
151 J. C. Jewett and C. R. Bertozzi, *Chem. Soc. Rev.*, 2010, **39**, 1272–1279.
152 B. A. H. Smith and C. R. Bertozzi, *Nat. Rev. Drug Discovery*, 2021, **20**, 217–243.
153 G. Ahn, N. M. Riley, R. A. Kamber, S. Wisnovsky, S. Moncayo von Hase, M. C. Bassik, S. M. Banik and C. R. Bertozzi, *Science*, 2023, **382**, eadf6249.
154 R. Vanella, A. Bazin, D. T. Ta and M. A. Nash, *Chem. Mater.*, 2019, **31**, 1899–1907.
155 A. Belluati, D. Happel, M. Erbe, N. Kirchner, A. Szelwicka, A. Bloch, V. Berner, A. Christmann, B. Hertel, R. Pardehkhorram, A. Reyhani, H. Kolmar and N. Bruns, *Nanoscale*, 2023, **15**, 19486–19492.
156 C. Jiao, C. Zhao, Y. Ma and W. Yang, *ACS Nano*, 2021, **15**, 15920–15929.
157 S. Lin, F. Wu, Y. Zhang, H. Chen, H. Guo, Y. Chen and J. Liu, *Chem. Soc. Rev.*, 2023, **52**, 6617–6643.
158 B. Hou, T. Zhang, H. Yang, X. Han, L. Liu, L. Li, C. Grazioli, X. Wu, N. Jiang and Y. Wang, *Interdiscip. Mater.*, 2023, **2**, 511–528.
159 W. Geng, L. Wang and X. Y. Yang, *Trends Biotechnol.*, 2022, **40**, 974–986.
160 A. Rodrigo-Navarro, S. Sankaran, M. J. Dalby, A. del Campo and M. Salmeron-Sanchez, *Nat. Rev. Mater.*, 2021, **6**, 1175–1190.

161 Z. Li, L. Xue, J. Yang, S. Wuttke, P. He, C. Lei, H. Yang, L. Zhou, J. Cao, A. Sinelshchikova, G. Zheng, J. Guo, J. Lin, Q. Lei, C. J. Brinker, K. Liu and W. Zhu, *Adv.Sci.*, 2024, **11**, 2305126.
162 L. Wen, G. Li, T. Huang, W. Geng, H. Pei, J. Yang, M. Zhu, P. Zhang, R. Hou, G. Tian, W. Su, J. Chen, D. Zhang, P. Zhu, W. Zhang, X. Zhang, N. Zhang, Y. Zhao, X. Cao, G. Peng, X. Ren, N. Jiang, C. Tian and Z. J. Chen, *Innovation*, 2022, **3**, 100342.
163 A. Noureddine, A. Maestas-Olguin, L. Tang, J. I. Corman-Hijar, M. Olewine, J. A. Krawchuck, J. Tsala Ebode, C. Edeh, C. Dang, O. A. Negrete, J. Watt, T. Howard, E. N. Coker, J. Guo and C. J. Brinker, *ACS Nano*, 2023, **17**, 16308–16325.
164 S. Guo, C. J. Brinker and W. Zhu, *Nat. Rev. Bioeng.*, 2024, **2**, 282–283.
165 Z. Sun, R. Hubner, J. Li and C. Wu, *Nat. Commun.*, 2022, **13**, 3142.
166 X. Wei, Y. Wang, Y. Liu, K. Ji, K. Li, J. Wang and Z. Gu, *Matter*, 2024, **7**, 826–854.
167 S. Pospich and S. Raunser, *Science*, 2017, **358**, 45–46.
168 Q. Lei, J. Guo, F. Kong, J. Cao, L. Wang, W. Zhu and C. J. Brinker, *J. Am. Chem. Soc.*, 2021, **143**, 6305–6322.
169 Y. Deng, T. Wu, X. Chen, Y. Chen, Y. Fei, Y. Liu, Z. Chen, H. K. Liang, J. J. Richardson, C. J. Doonan, X. Mulet, Y. Ju, J. Cui, F. Caruso and P. Falcaro, *Angew. Chem. Int. Ed.*, 2017, **56**, 8510–8515.
170 A. Kahana and D. Lancet, *Nat. Rev. Chem.*, 2021, **5**, 870–878.